

## Efficient and Accurate Double-Hybrid-Meta-GGA Density Functionals—Evaluation with the Extended GMTKN30 Database for General Main Group Thermochemistry, Kinetics, and Noncovalent Interactions

Lars Goerigk<sup>†,‡</sup> and Stefan Grimme<sup>\*,†</sup>

*Theoretische Organische Chemie, Organisch—Chemisches Institut der Universität  
Münster, Corrensstraße 40, and NRW Graduate School of Chemistry,  
Wilhelm-Klemm-Straße 10, D-48149 Münster, Germany*

Received August 18, 2010

**Abstract:** We present an extended and improved version of our recently published database for general main group thermochemistry, kinetics, and noncovalent interactions [*J. Chem. Theory Comput.* **2010**, 6, 107], which is dubbed GMTKN30. Furthermore, we suggest and investigate two new double-hybrid-meta-GGA density functionals called PTPSS-D3 and PWPB95-D3. PTPSS-D3 is based on reparameterized TPSS exchange and correlation contributions; PWPB95-D3 contains reparameterized PW exchange and B95 parts. Both functionals contain fixed amounts of 50% Fock-exchange. Furthermore, they include a spin-opposite scaled perturbative contribution and are combined with our latest atom-pairwise London-dispersion correction [*J. Chem. Phys.* **2010**, 132, 154104]. When evaluated with the help of the Laplace transformation algorithm, both methods scale as  $N^4$  with system size. The functionals are compared with the double hybrids B2PLYP-D3, B2GPPLYP-D3, DSD-BLYP-D3, and XYG3 for GMTKN30 with a quadruple- $\zeta$  basis set. PWPB95-D3 and DSD-BLYP-D3 are the best functionals in our study and turned out to be more robust than B2PLYP-D3 and XYG3. Furthermore, PWPB95-D3 is the least basis set dependent and the best functional at the triple- $\zeta$  level. For the example of transition metal carbonyls, it is shown that, mainly due to the lower amount of Fock-exchange, PWPB95-D3 and PTPSS-D3 are better applicable than the other double hybrids. Finally, we discuss in some detail the XYG3 functional [*Proc. Nat. Acad. Sci. U.S.A.* **2009**, 106, 4963], which makes use of B3LYP orbitals and electron densities. We show that it is basically a highly nonlocal variant of B2PLYP and that its partially good performance is mainly due to a larger effective amount of perturbative correlation compared to other double hybrids. We finally recommend the PWPB95-D3 functional in general chemistry applications.

### 1. Introduction

Kohn–Sham density functional theory (KS-DFT)<sup>1–5</sup> has become the “work-horse” of modern quantum chemistry. It represents a good compromise between computational effort and accuracy. Whenever costly wave function based methods

are not applicable to a certain kind of chemical problem, DFT provides a valuable alternative. However, the huge number of developed density functionals (DFs) to date shows that current approximate DFT still suffers from several flaws and that the quest for finding a functional, which comes close to the “true one”, is still ongoing. In this context, we want to particularly focus on the fact that not every DF is equally applicable to every problem (see, e.g., ref 6 for further information). This makes choosing the right functional for the right problem a tough task, even for experienced

\* Corresponding author phone: (+49)-251-8333241, e-mail: grimmes@uni-muenster.de.

<sup>†</sup> Universität Münster.

<sup>‡</sup> NRW Graduate School of Chemistry.

researchers in this field. Therefore, we think that the development of highly accurate and concomitantly robust, i.e., broadly applicable, DFs is very desirable.

In 2006, an important step toward this aim was the development of the B2PLYP double-hybrid density functional (DHDF),<sup>7</sup> which has its roots in the Görling–Levy Kohn–Sham perturbation theory.<sup>8,9</sup> It combines a standard hybrid-GGA DFT calculation with a second-order perturbative treatment based on KS orbitals, thus introducing nonlocal correlation effects or, in other words, information about virtual KS orbitals. For related precursors of this method, that mix wave function (WF) and DFT parts, see refs 10–12. Soon after, several variants of the double-hybrid idea were published.<sup>13–23</sup> The superior performance of double hybrids compared to common DFs was proven in many applications.<sup>24–40</sup>

The most recent study, showing the accuracy and robustness of B2PLYP, was at the same time the most thorough one. It was based on the so-called GMTKN24 database, which is a collection of 24 previously published or newly developed benchmark sets for general main group thermochemistry, kinetics, and noncovalent interactions.<sup>35</sup> It covers atomization energies, electron affinities, ionization potentials, proton affinities, self-interaction error (SIE) related problems, barrier heights, various reaction energies, particularly difficult cases for DFT methods, relative energies between conformers, and inter- and intramolecular noncovalent interactions. We pointed out that the range of properties covered by the GMTKN24 data set outperforms, to the best of our knowledge, all other combinations of databases that had been previously proposed. The GMTKN24 database's composition reflects many years of experience in benchmarking and in the application of DFT methods to “real-life” chemical problems. Our further positive experience with GMTKN24, since its publication, encouraged and confirmed our first impression that it is highly representative for chemistry (excluding transition metal compounds). Any quantum chemical method, that performs well for the entire database, can be really regarded as an accurate, robust, and useful method.

Since the publication of GMTKN24, we regarded six newly published benchmark sets as useful for giving further insight into a functional's applicability and performance.<sup>41–43</sup> Furthermore, recent developments and findings made it necessary to modify three of the original subsets.<sup>44,45</sup> Herein, we present the extended and modified version of GMTKN24, which is from now on called GMTKN30 and is recommended as a replacement.

With the help of GMTKN30, we want to re-evaluate the B2PLYP functional and want to compare the results with the recently published double hybrids B2GPPLYP,<sup>15</sup> DSD-BLYP,<sup>20</sup> and XYG3.<sup>21</sup> Furthermore, we also present two new DHDFs, called PTPSS and PWPB95, which are not based on hybrid-GGA but on hybrid-meta-GGA ingredients. For these two DHDFs, the perturbative treatment is carried out within a spin-opposite scaled (SOS) scheme.<sup>46,47</sup> When combined with a Laplace transformation algorithm,<sup>48</sup> this reduces the formal computational cost from  $N^5$ , with  $N$  being the system size, to  $N^4$ , which is then formally the same as

the scaling of common hybrid DFs. Similar ideas have recently been proposed by Scuseria et al. in the framework of a truncated random phase approximation ansatz combined with long-range corrected DFT parts (LC- $\omega$ LDA+JMP2).<sup>49</sup>

This manuscript is structured as follows. First, the extended GMTKN30 database is presented. Second, the background of double-hybrid density functional theory will be discussed, with an emphasis on the XYG3 variant, and the new PTPSS and PWPB95 methods. Together with B2PLYP, B2GPPLYP, and DSD-BLYP, these methods are then benchmarked against GMTKN30. Moreover, we want to give an impression of the functionals' performance for transition metal chemistry with the example of carbonyl dissociation reactions. Furthermore, we will suggest a new scheme with which to determine the  $s_6$  scale parameter of the DFT-D3 correction for DHDFs. We will also study basis set effects, address critical points recently raised against the DHDF formalism,<sup>45,21,22,50</sup> and shed some light on the XYG3 approach.

## 2. The GMTKN30 Data Set

The recently presented GMTKN24 database for general main group thermochemistry, kinetics, and noncovalent interactions covers a large variety of 24 different, chemically relevant subsets.<sup>35</sup> Here, we present an extended version with six new and three modified subsets. This extended database is called GMTKN30. In Table 1, short descriptions for each part of the GMTKN30 database are given, including the number of entries, a specification of the reference values, and the relevant citations. Note that none of the reference data include zero point vibrational energies (ZPVEs) or thermal (enthalpic) corrections. The type and source of reference data are given separately for each subset. In total, the GMTKN30 database comprises 1218 single point calculations and 841 data points (relative energy values). In Figure 1, an overview of the six additional subsets is given. For each set, the, on average, easiest and most difficult reactions (for GGA functionals) are shown. The reference values and the optimized coordinates of all systems are available for download from our Web site.<sup>51</sup> A detailed description of the original GMTKN24 subsets is given in ref 35. In the following, only the changes and additions to the original database are described.

**2.1. The Modified NBPRC Subset.** For the GMTKN24 database, a completely new benchmark set, called NBRC, was introduced.<sup>35</sup> It contained six oligomerization and dihydrogen fragmentation reactions of ammonia/borane systems. The reason for creating such a set was previous evidence of poor performance for similar reactions for some popular density functionals like B3LYP (see, e.g., ref 52). Recently, we investigated the mechanism of  $H_2$  activation by frustrated Lewis pairs (FLPs).<sup>44</sup> In order to validate the theoretical methods used in that study, a small benchmark set for  $H_2$  activation by three FLP-like model systems was developed:

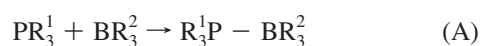


**Table 1.** Description of the Subsets within the GMTKN30 Database (New or Modified Subsets Are Emphasized in Italics)

set	description	#	av. $ \Delta E ^a$	ref method	reference
MB08-165	decomposition energies of artificial molecules	165	117.2	est. CCSD(T)/CBS	<i>b</i>
W4-08	atomization energies of small molecules	99	237.5	W4	<i>c</i>
W4-08woMR	W4-08 without multireference cases	83	261.5	W4	<i>c</i>
G21IP	adiabatic ionization potentials	36	250.8	exp.	<i>d</i>
G21EA	adiabatic electron affinities	25	33.6	exp.	<i>d</i>
PA	adiabatic proton affinities	12	174.9	est. CCSD(T)/CBS and W1	<i>e, f</i>
SIE11	self-interaction error related problems	11	34.0	est. CCSD(T)/CBS	<i>g</i>
BHPERI	barrier heights of pericyclic reactions	26	19.4	W1 and CBS-QB3	<i>c, h, i, j, k</i>
BH76	barrier heights of hydrogen transfer, heavy atom transfer, nucleophilic substitution, unimolecular, and association reactions	76	18.5	W1 and theor. est.	<i>l, m</i>
BH76RC	reaction energies of the BH76 set	30	21.5	W1 and theor. est.	<i>l, m</i>
RSE43	radical stabilization energies	43	7.5	est. CCSD(T)/CBS	<i>n</i>
O3ADD6	reaction energies, barrier heights, association energies for addition of O <sub>3</sub> to C <sub>2</sub> H <sub>4</sub> and C <sub>2</sub> H <sub>2</sub>	6	22.7	est. CCSD(T)/CBS	<i>o</i>
G2RC	reaction energies of selected G2/97 systems	25	50.6	exp.	<i>p</i>
AL2X	dimerization energies of AlX <sub>3</sub> compounds	7	33.9	exp.	<i>q</i>
NBPRC	oligomerizations and H <sub>2</sub> fragmentations of NH <sub>3</sub> /BH <sub>3</sub> systems; H <sub>2</sub> activation reactions with PH <sub>3</sub> /BH <sub>3</sub> systems	12	27.3	est. CCSD(T)/CBS	<i>g, r</i>
ISO34	isomerization energies of small and medium-sized organic molecules	34	14.3	exp.	<i>s</i>
ISOL22	isomerization energies of large organic molecules	22	18.3	SCS-MP3/CBS	<i>t</i>
DC9	nine difficult cases for DFT	9	35.7	theor. and exp.	<i>g, j, u, v, w, x, y, z</i>
DARC	reaction energies of Diels–Alder reactions	14	32.2	est. CCSDT/CBS	<i>q</i>
ALK6	fragmentation and dissociation reactions of alkaline and alkaline–cation–benzene complexes	6	44.6	est. CCSD(T)/CBS	<i>aa</i>
BSR36	bond separation reactions of saturated hydrocarbons	36	16.7	est. CCSD(T)/CBS	<i>bb</i>
IDISP	intramolecular dispersion interactions	6	13.5	theor. and exp.	<i>s, cc, dd, this work</i>
WATER27	binding energies of water, H <sup>+</sup> (H <sub>2</sub> O) <sub>n</sub> and OH <sup>−</sup> (H <sub>2</sub> O) <sub>n</sub> clusters	27	82.0	est. CCSD(T)/CBS; MP2/CBS	<i>ee</i>
S22	binding energies of noncovalently bound dimers	22	7.3	est. CCSD(T)/CBS	<i>ff, gg</i>
ADIM6	interaction energies of <i>n</i> -alkane dimers	6	3.3	est. CCSD(T)/CBS	<i>aa</i>
RG6	interaction energies of rare gas dimers	6	0.46	exp.	<i>aa, hh, ii, jj, kk</i>
HEAVY28	noncovalent interaction energies between heavy element hydrides	28	1.3	est. CCSD(T)/CBS	<i>aa</i>
PCONF	relative energies of phenylalanyl–glycyl–glycine tripeptide conformers	10	1.5	est. CCSD(T)/CBS	<i>ll</i>
ACONF	relative energies of alkane conformers	15	1.8	W1h-val	<i>mm</i>
SCONF	relative energies of sugar conformers	17	4.9	est. CCSD(T)/CBS	<i>g, nn</i>
CYCONF	relative energies of cysteine conformers	10	2.1	est. CCSD(T)/CBS	<i>oo</i>

<sup>a</sup> Averaged absolute energies in kcal mol<sup>−1</sup>, excluding ZPVEs. <sup>b</sup> Ref 31. <sup>c</sup> Ref 15. <sup>d</sup> Ref 116. <sup>e</sup> Ref 117. <sup>f</sup> Ref 118. <sup>g</sup> Ref 34. <sup>h</sup> Ref 119. <sup>i</sup> Ref 120. <sup>j</sup> Ref 25. <sup>k</sup> Ref 121. <sup>l</sup> Ref 122. <sup>m</sup> Ref 123. <sup>n</sup> Ref 124. <sup>o</sup> Ref 125. <sup>p</sup> Ref 126. <sup>q</sup> Ref 127. <sup>r</sup> Ref 43. <sup>s</sup> Ref 60. <sup>t</sup> Ref 40. <sup>u</sup> Ref 128. <sup>v</sup> Ref 129. <sup>w</sup> Ref 130. <sup>x</sup> Ref 131. <sup>y</sup> Ref 132. <sup>z</sup> Ref 7. <sup>aa</sup> Ref 42. <sup>bb</sup> Ref 41. <sup>cc</sup> Ref 23. <sup>dd</sup> Ref 55. <sup>ee</sup> Ref 133. <sup>ff</sup> Ref 58. <sup>gg</sup> Ref 44. <sup>hh</sup> Ref 66. <sup>ii</sup> Ref 67. <sup>jj</sup> Ref 68. <sup>kk</sup> Ref 69. <sup>ll</sup> Ref 134. <sup>mm</sup> Ref 135. <sup>nn</sup> Ref 136. <sup>oo</sup> Ref 137.



Reaction A describes the formation of the Lewis pairs, whereas B is their reaction with H<sub>2</sub>. We considered three reactions A and B with R<sup>1</sup> = H/R<sup>2</sup> = H, R<sup>1</sup> = CH<sub>3</sub>/R<sup>2</sup> = F, and R<sup>1</sup> = CH<sub>3</sub>/R<sup>2</sup> = Cl. Geometries for these model reactions were obtained at the B3LYP-D/TZVP level of theory. Estimated CCSD(T)/CBS reference values for these reactions were obtained as proposed by Jurecka and Hobza.<sup>53</sup> MP2/CBS<sup>54</sup> values (based on cc-pVTZ and cc-pVQZ results) were corrected by the difference of CCSD(T)/cc-pVTZ and MP2/cc-pVTZ correlation energies. We added these reactions to the original set and dubbed the new set NBPRC. In order to calculate all reaction energies of NBPRC, 21 single point calculations have to be carried out. The energy range is from −48.3 to +40.4 kcal/mol. The average absolute reaction energy is 27.3 kcal/mol.

**2.2. Changes to the IDISP Subset.** The original IDISP subset for intramolecular London-dispersion effects of six large organic systems involves 13 single point calculations and has an average relative energy of 14.1 kcal/mol.<sup>35</sup> In three cases, we felt it necessary to recalculate the reference

values. The original reference value of 9.4 kcal/mol for the isomerization of *n*-undecane to 2,2,3,3,4,4-hexamethylpentane was based on the SCS-MP2/cQZV3P//MP2/TZVP level of theory.<sup>55</sup> We found significant differences between MP2/CBS (3.9 kcal/mol) and SCS-MP2/CBS (10.0 kcal/mol) treatments (based on aug-cc-pVTZ → aug-cc-pVQZ extrapolations). Thus, we decided to base the new value on MP2.5; i.e., an MP2/CBS energy is combined with one-half of the third-order contribution of MP3/aug-cc-pVDZ (carried out with the group's own program RICC<sup>56</sup>). MP2.5 had been shown to yield accurate results that are in some cases even comparable to a CCSD(T)/CBS treatment.<sup>57</sup> The new reference value is 8.2 kcal/mol. Furthermore, the reference values for the folding of the C<sub>14</sub>H<sub>30</sub> and C<sub>22</sub>H<sub>46</sub> hydrocarbons were recalculated. Originally, the values of −2.2 and +3.6 kcal/mol were based on MP2/aug-cc-pVTZ//BLYP-D/TZV(p,d) calculations.<sup>24</sup> However, according to MP2/CBS results, convergence to about 0.5 kcal/mol accuracy is only obtained after aug-cc-pVTZ → aug-cc-pVQZ extrapolations. The new values are −3.1 and +0.4 kcal/mol, respectively. Because of the new reference values, the average relative energy for

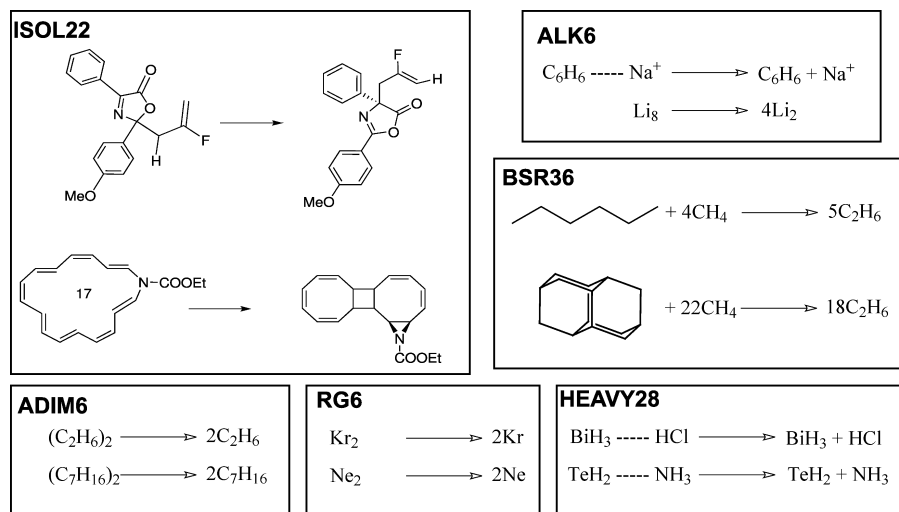


**Figure 1.** The six new subsets of the GMTKN30 database. For each set, the, on average, easiest (top) and most difficult (bottom in each box) reactions (for GGAs) are shown.

the complete subset changes to 13.5 kcal/mol. The energy range is from  $-58.5$  to  $+8.2$  kcal/mol.

**2.3. New Reference Values for the S22 Set.** Hobza and co-workers derived the reference values for the 22 interaction energies of noncovalently bound complexes (S22 set) within an estimated CCSD(T)/CBS scheme.<sup>58</sup> However, as Sherrill and co-workers argued, both MP2/CBS values and the differences between CCSD(T) and MP2 correlation energies were based on various basis sets for different systems and, thus, are not consistent throughout the set. Therefore, they recently estimated new CCSD(T)/CBS data.<sup>45</sup> Shortly after that publication, Podeszwa et al. also proposed new reference values.<sup>59</sup> We considered both proposals carefully and found the two sets of new reference values to be almost identical. We will use the energies published by Sherrill and co-workers. With these revised values, the S22 set has an average absolute interaction energy of 7.3 kcal/mol. The energy range is from 0.5 to 20.7 kcal/mol.

**2.4. The ISOL22 Subset.** Very recently, Huenerbein et al. published a new benchmark set containing 24 isomerization reactions (ISOL<sup>41</sup>) of large molecules covering a wide range of different compounds, like, e.g., a sugar, a steroid, an organic dye, hydrocarbons, and large molecules containing heteroatoms. In contrast to the popular ISO34 set,<sup>60</sup> which is also a part of GMTKN24 and GMTKN30, the large size of the molecules casts an additional light on effects that are important in “real life” organic chemistry. These are, in particular, intramolecular London-dispersion effects. Furthermore, charged systems are also considered. Reference values are based on the SCS-MP3/CBS//B97-D/TZVP levels of theory. For the present study, we excluded reactions 1 and 4 (see ref 41 for more details) as treating them is very time-consuming and not feasible in an extensive benchmark study. Thus, the subset presented herein contains only 22 reactions (44 single point calculations) and is called ISOL22. The energy range is from 0.5 to 38.1 kcal/mol. The average reaction energy is 18.3 kcal/mol.

**2.5. ALK6.** For the development of the new London-dispersion correction termed DFT-D3, Grimme et al. introduced the so-called ALK6 benchmark set that includes three

decomposition reactions of alkaline metal complexes  $\text{M}_8$  ( $\text{M} = \text{Li}, \text{Na}, \text{K}$ ) into their dimers and three dissociation reactions of alkaline-cation–benzene complexes  $\text{M}^+ - \text{Bz}$ .<sup>43</sup> Reference values are based on estimated CCSD(T)/CBS calculations. The complete set comprises 13 single point calculations, and its average reaction energy is 44.6 kcal/mol. The energy range is from 19.2 to 83.2 kcal/mol.

**2.6. The BSR36 Subset.** Recently, Steinmann et al.<sup>61</sup> carried out a dispersion corrected density functional study on 36 bond separation reactions (as introduced by Pople and co-workers<sup>62,63</sup> and also recently investigated by Wodrich et al.<sup>64</sup>). These are reactions of different saturated hydrocarbons [15 (partially branched) chains, five cages, and 16 rings] with methane to yield ethane. As reference values, experimental heats of formation were taken. However, Krieg and Grimme revealed that usage of these reference values led to misleading interpretations regarding different density functionals.<sup>42</sup> They concluded that a theoretical reference is more appropriate for this test set and computed reaction energies on the estimated CCSD(T)/CBS//MP2/cc-pVTZ level of theory. The complete test set was dubbed BSR36. The set comprises 38 single point calculations and has an average reaction energy of 16.7 kcal/mol. The energy range is from 2.4 to 51.4 kcal/mol.

**2.7. The ADIM6 Subset.** Tsuzuki et al. published estimated CCSD(T)/CBS reference values for the interaction energies of *n*-alkane dimers ( $n = 1-10$ ).<sup>65</sup> Grimme et al. took the systems with  $n = 2-7$  for their study of the new London-dispersion correction and called this benchmark set ADIM6.<sup>42</sup> ADIM6 involves 12 single point calculations and has an average interaction energy of 3.3 kcal/mol. The energy range is from 1.3 to 5.6 kcal/mol.

**2.8. The RG6 Subset.** Grimme et al. used (partially theoretically corrected) experimental<sup>66-69</sup> dissociation energies of five homonuclear and one heteronuclear rare gas dimer for the development of DFT-D3.<sup>43</sup> This subset was denoted RG6. It involves 11 single point calculations and has an average dissociation energy of 0.46 kcal/mol. The energy range is from 0.08 to 0.79 kcal/mol.



**2.9. The HEAVY28 Subset.** The HEAVY28 benchmark set by Grimme et al. comprises 28 noncovalent interaction energies of different heavy element hydrides (e.g., including hydrides of Sb, Te, I, Pb, and Bi).<sup>43</sup> Reference values are based on estimated CCSD(T)/CBS calculations. Thirty-eight single point calculations are carried out for the evaluation of HEAVY28. The energy range is from 0.44 to 3.29 kcal/mol. Its average interaction energy is 1.31 kcal/mol.

**2.10. Weighted Total Mean Absolute Deviation.** In our recent study, we completed the analysis of the GMTKN24 database using an overall statistical evaluation. In the spirit of the work by Truhlar and co-workers (see, e.g., ref 70), we defined a weighted total mean absolute deviation (WT-MAD) to combine all obtained mean absolute deviations (MADs) for each subset into one final number for a tested method. We also discussed that such a procedure can be defined in several ways and that there is no real right or wrong. After having tested several schemes, we found that the overall ranking of methods was not altered. In the scheme, which we finally presented (see eq 1), each of 24 MAD values was weighted by the number of entries ( $N_i$ ) of each subset to take into account its size. Furthermore, each subset was weighted by an additional factor that was calculated as the ratio between the MADs of BLYP and B2PLYP-D [i.e.,  $\text{MAD}(\text{BLYP})/\text{MAD}(\text{B2PLYP-D})$ ] to take into account the difficulty of a certain subset.

$$\text{WTMAD} = \frac{1}{3091.4} \times \sum_i^{30} N_i \times \frac{\text{MAD}_i^{\text{BLYP}}}{\text{MAD}_i^{\text{B2PLYP-D}}} \times \text{MAD}_i \quad (1)$$

In order to be consistent, and although we will apply the new DFT-D3 correction in the present study, we decided to define the WTMAD for GMTKN30 in the same way, i.e., with the older version DFT-D. The only difference is that we introduced the additional constraint that the product of system size and scale factor of a certain set should not be larger than one-half of the corresponding value for MB08-165, i.e., 222.75. Therefore, it is guaranteed that smaller sets with a large scale factor enter not too strongly. The actual values for the weighting factors of all 30 subsets are given in the Supporting Information.

### 3. Double-Hybrid Density Functional Theory

Double-hybrid density functionals (DHDFs) are situated on the fifth rung in Perdew's scheme of "Jacob's ladder"<sup>71</sup> as they include virtual Kohn–Sham orbitals (here, we also want to acknowledge that the closely related term "doubly hybrid" originated from Truhlar and co-workers' multicoefficient methods<sup>10,11</sup>). Compared to hybrid-GGA functionals (fourth rung), where some part of the exchange functional is substituted by "exact" (HF) exchange, DHDFs additionally substitute some part of the correlation functional by mixing in a nonlocal perturbative correlation. This correlation part is basically obtained by a second-order Møller–Plesset (MP2) type treatment based on KS orbitals and eigenvalues. The first DHDF following this idea is the B2PLYP functional of Grimme,<sup>7</sup> which was soon followed by the mPW2PLYP functional of Schwabe and Grimme.<sup>13</sup> B2PLYP is nowadays

a widely recognized functional, which, in combination with an empirical London-dispersion term (DFT-D<sup>72</sup>/DFT-D3<sup>43</sup>), resulted in being very accurate and robust in several ground- and excited-state studies.<sup>24–40,43</sup> This stimulated further works, and several modifications of B2PLYP were proposed in recent years. These are the B2KPLYP, B2TPLYP, and B2GPPLYP variants by Martin and co-workers, specifically designed as functionals working well for kinetics, thermochemistry, and general purpose applications.<sup>14,15</sup> The reparameterized B2 $\pi$ -PLYP functional of Sancho-García and Pérez-Jiménez was developed to work particularly well in  $\pi$ -conjugated systems.<sup>16</sup> Head-Gordon and co-workers proposed a distance-dependent scaling of the perturbative correlation part and developed the variants B2P3LYP and B2OS3LYP.<sup>17</sup> The latter functional includes perturbative contributions of electron pairs with opposite spins only (in the spirit of the SOS-MP2<sup>47</sup> method). Radom and co-workers proposed a reparameterized restricted open-shell version, dubbed RO-B2PLYP, for the treatment of open-shell systems.<sup>18</sup> The very recently published DSD-BLYP functional by Kozuch et al. is a spin-component-scaled variant of the B2(GP)PLYP approaches, including the DFT-D dispersion correction.<sup>20</sup> Other recently developed DHDFs are the long-range corrected  $\omega$ B97X-2 of Chai and Head-Gordon,<sup>19</sup> the XYG3 method of Zhang et al.,<sup>21</sup> and its modified versions XYG3s<sup>22</sup> and XYG3o.<sup>23</sup> An overview of the different double-hybrid approaches is given in Table 2.

In this study, we will investigate the B2PLYP, B2GPPLYP, DSD-BLYP, and XYG3 DHDFs together with our newly proposed methods PTPSS and PWPB95.

**3.1. The B2PLYP and B2GPPLYP Functionals.** B2PLYP and B2GPPLYP follow the same idea and just differ by amounts of Fock-exchange and perturbative correlation mixing. The first step in a B2(GP)-PLYP calculation is the generation of Kohn–Sham orbitals from the hybrid-GGA portion of the DHDF, which is denoted B2LYP or B2GPLYP (eq 2).

$$E_{\text{XC}}^{\text{B2(GP)LYP}} = (1 - a_{\text{X}})E_{\text{X}}^{\text{B88}} + a_{\text{X}}E_{\text{X}}^{\text{HF}} + (1 - a_{\text{C}})E_{\text{C}}^{\text{LYP}} \quad (2)$$

The hybrid-GGA part contains the Becke 1988 (B88)<sup>73</sup> exchange  $E_{\text{X}}^{\text{B88}}$  combined with nonlocal Fock-exchange  $E_{\text{X}}^{\text{HF}}$  and Lee–Yang–Parr (LYP)<sup>74,75</sup> correlation  $E_{\text{C}}^{\text{LYP}}$ . The  $a_{\text{X}}$  and  $a_{\text{C}}$  are mixing parameters for the "exact" Fock-exchange and perturbative correlation, respectively. A second-order perturbation treatment (PT2), based on the KS orbitals and eigenvalues resulting from the B2(GP)LYP calculation, is carried out yielding the correlation energy  $E_{\text{C}}^{\text{PT2}}$  that is scaled by the mixing parameter  $a_{\text{C}}$ . Although Brillouin's theorem is not valid, only double excitations from the KS determinant are considered. Single contributions are neglected and indirectly accounted for by the fitted scaling parameters. Thus, the final form of the B2(GP)PLYP exchange correlation energy is given by

$$E_{\text{XC}}^{\text{B2(GP)PLYP}} = E_{\text{XC}}^{\text{B2(GP)-LYP}} + a_{\text{C}}E_{\text{C}}^{\text{PT2}} \quad (3)$$

In the case of B2PLYP, the two mixing parameters were fitted to the heats of formation (HOFs) of the G2/97 set by

**Table 2.** Overview of Various Double-Hybrid Density Functionals

functional	description	ref
B2PLYP	B88 exchange; LYP correlation; PT2 correlation based on hybrid-GGA part	ref 7
mPW2PLYP	like B2PLYP, but with mPW exchange	ref 13
B2KPLYP	reparameterized B2PLYP version for kinetics	ref 14
B2TPLYP	reparameterized B2PLYP version for thermochemistry	ref 14
B2GPPLYP	reparameterized B2PLYP version for general purpose applications	ref 15
B2 $\pi$ PLYP	reparameterized B2PLYP version for conjugated $\pi$ -systems	ref 16
B2P3LYP	modified B2PLYP version with long-range PT2 correction	ref 17
B2OS3LYP	similar to B2P3LYP, but with SOS-PT2 correlation	
ROB2PLYP	reparameterized B2PLYP version within an ROKS formalism for treating open-shell systems	ref 18
$\omega$ B97X-2	ingredients of the B97 functional; long-range corrected; SCS-PT2 correlation	ref 19
XYG3	B88 exchange; LYP correlation; evaluated with B3LYP orbitals and densities	ref 21
XYG3s/XYG3o	modified XYG3 versions to account for basis set incompleteness	refs 22 and 23
DSD-BLYP	modified B2PLYP version with SCS-PT2 correction; fitted together with DFT-D dispersion correction	ref 20
PTPSS	reoptimized TPSS exchange and correlation; SOS-PT2 correlation; fitted together with DFT-D3 dispersion correction	this work
PWPB95	reoptimized PW exchange and B95 correlation; SOS-PT2 correlation; fitted together with DFT-D3 dispersion correction	this work

using a basis of quadruple- $\zeta$  quality (QZV3P). The parameters are  $a_X = 0.53$  and  $a_C = 0.27$ . The parameters of B2GPPLYP were determined after taking into consideration atomization energies and reaction barrier heights by using the aug-pc2 and aug-pc3 basis sets. B2GPPLYP contains larger amounts of Fock-exchange ( $a_X = 0.65$ ) and perturbative correlation ( $a_C = 0.36$ ) than B2PLYP. It has been noted that these two double hybrids still lack an asymptotically correct description of long-range London-dispersion effects ( $a_C < 1$ ), although the inclusion of the nonlocal PT2 part already leads to a qualitatively better description compared to common DFs. Therefore, it was suggested to combine the functionals with an empirical London-dispersion correction (DFT-D).<sup>24</sup>

Very recently, our group proposed a new version of this correction called DFT-D3, and we will make use of it in the present study.<sup>43</sup> Compared to the previously published versions,<sup>72,76</sup> DFT-D3 contains more “ab initio” ingredients and is characterized by less empiricism. It also contains system-specific  $C_6$  and  $C_8$  parameters, depending on the coordination sphere of each atom within a molecule. More details about this correction can be found in ref 43. In the present context, it is only necessary to mention that the dispersion correction  $E_{\text{disp}}$  includes two atom-pairwise terms:

$$E_{\text{disp}} = - \sum_{\text{AB}} \left( s_6 f_{\text{d},6}(R_{\text{AB}}, s_{\text{r},6}) \frac{C_6^{\text{AB}}}{R_{\text{AB}}^6} + s_8 f_{\text{d},8}(R_{\text{AB}}) \frac{C_8^{\text{AB}}}{R_{\text{AB}}^8} \right) \quad (4)$$

where  $R_{\text{AB}}$  is the distance between two atoms A and B in a chemical system. The asymptotically relevant dipole–dipole term is scaled by a parameter  $s_6$  and additionally contains a second parameter  $s_{\text{r},6}$ , which scales cutoff radii within the damping function  $f_{\text{d},6}$ . The second term is proportional to  $R_{\text{AB}}^{-8}$  and scaled by a factor  $s_8$ . For common DFs,  $s_6$  is set to unity to ensure that the DFT-D3 correction has a physically correct asymptotic behavior. The other two parameters are fitted to a set of 130 noncovalent interaction energies. For double hybrids, an  $s_6$  value smaller than unity has to be chosen, because of the presence of the nonlocal PT2 contribution. For B2PLYP,  $s_6$  was originally set to 0.5.<sup>77</sup>

However, herein, we introduce a new scheme to estimate the  $s_6$  value. We consider the three rare gas dimers  $\text{Ne}_2$ ,  $\text{Ar}_2$ ,

and  $\text{Kr}_2$  at large distances at which only long-range dispersion plays a role (7 Å for the neon dimer and 10 Å for the other two systems). The dispersion energies [i.e.,  $E_{\text{disp}}^{\text{CCSD(T)}} = E_{\text{corr}}^{\text{CCSD(T)}}(\text{dimer}) - 2E_{\text{corr}}^{\text{CCSD(T)}}(\text{monomer})$ ] for these systems were then estimated at the CCSD(T)<sup>78</sup>/aug-cc-pVTZ<sup>79</sup> level of theory (carried out with Molpro 2009.1<sup>80</sup>), for which an asymptotically correct  $R_{\text{AB}}^{-6}$  behavior is expected. With the same basis set, the scaled perturbative dispersion energy of the considered DHDF ( $E_{\text{disp}}^{\text{PT2}}$ ) is computed and compared to that of the coupled cluster treatment as the ratio between both dispersion energies ( $E_{\text{disp}}^{\text{PT2}}/E_{\text{disp}}^{\text{CCSD(T)}}$ ). Finally, the average is taken over the three systems. To obtain the actual  $s_6$  value, this average is subtracted from unity. Thus, an ideal method that correctly describes long-range dispersion interactions should have an  $s_6$  of zero.

To validate our approach, we made some preliminary checks with the MP2, SCS-MP2, and SOS-MP2 methods. The MP2 method underestimates the CCSD(T) energy by 15% for  $\text{Ne}_2$  but overestimated it by 10 and 18% for  $\text{Ar}_2$  and  $\text{Kr}_2$  (see Table S1 in the Supporting Information). On average, it gives a slight overestimation in the asymptotic limit, and thus the  $s_6$  value is by  $-0.04$  slightly negative. This overestimation is in accordance with previous observations (see, e.g., refs 20, 81, 82). The SCS-MP2 and SOS-MP2 methods underestimate the dispersion energies for all dimers and have  $s_6$  values of 0.18 and 0.30, respectively. If the spin-opposite scale parameter of SOS-MP2 is set to unity, we obtain  $s_6 = 0.47$ , which is close to the expected value of one-half (in the asymptotic range, both the same and opposite spin parts have the same contributions).

After validating our approach, the  $s_6$  value of B2PLYP was determined to be 0.64, which is larger than originally proposed. The other two parameters  $s_{\text{r},6}$  and  $s_8$  were then refitted as described above and in the DFT-D3 paper. Following the same procedure, the  $s_6$  value of B2GPPLYP turned out to be 0.56. The resulting values for  $s_{\text{r},6}$  and  $s_8$  for both functionals are given in Table 3. More information about the results for the fit set used to determine the parameters can be found on our Web site.<sup>51</sup> It is recommended to use these revised parameters in future B2(GP)PLYP-D3 applications.

**3.2. The DSD-BLYP Functional.** The very recently published DSD-BLYP<sup>20</sup> functional is closely related to the

**Table 3.** Parameters for the DFT-D3 Correction

method	$s_6$	$s_{r,6}$	$s_8$
B2PLYP	0.64	1.427	1.022
B2GPPLYP	0.56	1.586	0.760
DSD-BLYP	0.50	1.569	0.705
PTPSS	0.75	1.541	0.879
PWPB95	0.82	1.557	0.705

B2(GP)PLYP approaches. It also contains B88 exchange and LYP correlation. However, the perturbative part is now based on the spin-component scaling idea (SCS-PT2).<sup>46</sup> The two scaling parameters ( $c_O$  and  $c_S$ ) for the opposite ( $E_C^{OS-PT2}$ ) and same-spin contributions ( $E_C^{SS-PT2}$ ) are, moreover, independent from the scaling parameter ( $c_C$ ) of the LYP correlation portion:

$$E_{XC}^{DSD-BLYP} = E_X^{B88} + a_X E_X^{HF} + c_C E_C^{LYP} + c_O E_C^{OS-PT2} + c_S E_C^{SS-PT2} \quad (5)$$

The three correlation scaling parameters and the amount of Fock-exchange were determined with a training set covering atomization energies, reaction barriers, noncovalently bound systems, transition metal compounds, and the MB08-186 set, which is also part of GMTKN30. Various basis sets of triple- and quadruple- $\zeta$  quality were used for this purpose. With an  $a_X$  value of 0.69, DSD-BLYP contains even more Fock-exchange than B2GPPLYP. The three correlation scale parameters are  $c_C = 0.54$ ,  $c_O = 0.46$ , and  $c_S = 0.37$ . During the fitting procedure, the old DFT-D correction was applied, and the  $s_6$  value was also fitted. In this work, we will make use of the DSD-BLYP functional, without changing the parameters. However, we will apply the new DFT-D3 correction and will refer to this combination as DSD-BLYP-D3. The three parameters were determined as described above for B2(GP)PLYP and are given in Table 3.

**3.3. The XYG3 Functional.** The XYG3 functional represents a different kind of B2PLYP variant. Instead of self-consistently creating the KS orbitals from the DHDF's hybrid-GGA part, the authors proposed to carry out first a normal B3LYP calculation. The resulting orbitals and density are used to evaluate both the empirically adjusted hybrid-GGA part (nonself-consistently) and the PT2 energy. When starting to work with the XYG3 functional, we had some problems with its implementation. We followed the author's description in the XYG3 paper.<sup>21</sup> According to them, the XYG3 formula reads

$$E_{XC}^{XYG3} = E_X^S + E_C^{VWN} + a_X(E_X^{HF} - E_X^S) + a_0 \Delta E_X^{B88} + a_C(E_C^{PT2} - E_C^{LYP}) + (1 - a_C) \Delta E_C^{LYP} \quad (6)$$

where  $E_X^{Slater}$  stands for Slater exchange,<sup>83</sup>  $E_C^{VWN}$  for the VWN-LDA correlation,<sup>84</sup>  $\Delta E_X^{B88}$  for the gradient correction part of the B88 functional, and  $\Delta E_C^{LYP}$  for the gradient correction part of LYP [note that in later publications the factor  $(1 - a_C)$  is missing before  $\Delta E_{LYP}$ ].<sup>22,23,50</sup> The reason for our problems seems to be the 100% of VWN correlation that is mixed in. In fact, we were not able to reproduce the results published in the XYG3 paper. However, we found

another description of the XYG3 functional in a recent study by Vázquez-Mayagoitia et al.<sup>85</sup> that does not include VWN correlation. With that description, we were able to reproduce the results of the original XYG3 paper. This, apparently correct, formula reads

$$E_{XC}^{XYG3} = a_X E_X^{HF} + (1 - a_X) E_X^S + a_0 \Delta E_X^{B88} + (1 - a_C) E_C^{LYP} + a_C E_C^{PT2} \quad (7)$$

In principle, XYG3 contains the same ingredients as B2PLYP and B2GPPLYP, with the exception that a different scaling of the LDA and semilocal exchange parts is applied. The three scale parameters  $a_X$ ,  $a_0$ , and  $a_C$  were determined by a fit to the thermochemical data in the G3/99 set by applying the 6-311+G(3df,2p) basis ( $a_X = 0.8033$ ,  $a_0 = 0.2107$ , and  $a_C = 0.3211$ ). Thus, XYG3 is the DHDF with the largest amount of Fock-exchange (80.33%). We will later comment on the magnitude of the PT2 part in XYG3. Because the orbitals and density result from a different functional (e.g., B3LYP in XYG3) than the final semilocal exchange-correlation parts, XYG3 also contains an additional empirical degree of freedom compared to the other DHDFs.

**3.4. The PTPSS Functional.** The herein proposed PTPSS density functional ("P" stands for "perturbative") differs basically in four ways from B2PLYP and related methods. First of all, the key ingredients, i.e., the semilocal DFT parts, are changed from B88 exchange and LYP correlation to TPSS<sup>86</sup> exchange and correlation. Thus, PTPSS is a double-hybrid-meta-GGA functional given by

$$E_{XC}^{PTPSS} = (1 - a_X) E_X^{TPSS} + a_X E_X^{HF} + (1 - a_C) E_C^{TPSS} + a_C E_C^{OS-PT2} \quad (8)$$

The second major difference is that only contributions of electron pairs with opposite spin (OS) are included for the perturbative part  $E_C^{OS-PT2}$ , similar to the B2OS3LYP functional. This brings the formal scaling of  $N^5$  with system size down to  $N^4$ , due to a Laplace transformation algorithm,<sup>48</sup> as first shown for the SOS-MP2 method.<sup>47</sup> We observed that by just neglecting the same spin (SS) terms, the errors for our fit set (see below) were reduced drastically. It is important to note here that PTPSS is only competitive at this SOS-PT2 level, while this is different with the B88/LYP parts where the same spin part must be included. This observation is consistent with the fact that (a) LYP does not contain any same-spin correlation, meaning that it must be considered by PT2 in a LYP-based DHDF, and (b) the same-spin correlation energy is not as accurate as the OS contribution at second order, as indicated by the success of SCS-MP2.<sup>46</sup> Thus, when the same spin part is already described well at the semilocal level by, e.g., TPSS, it seems better to neglect it in the PT2 treatment also to avoid double-counting effects entirely.

The third difference is that in previously published DHDFs only the scale factors for the Fock-exchange and perturbative correlation were fitted, whereas the semilocal DF parameters (e.g.,  $\beta$  in B88) remained unchanged. Very recently, we discovered that the results with the TPSS ansatz improve significantly and become comparable to some results of



hybrid-GGA DFs when the seven parameters are refitted (termed oTPSS, where the prefix “o” stands for “optimized”).<sup>35</sup> This observation inspired us in the first place to develop a double-hybrid based on TPSS, for which also these seven parameters are adjusted.

The TPSS exchange functional has the following form:

$$E_X^{\text{TPSS}} = \sum_{\sigma} \int \rho \varepsilon_X^{\text{LDA}} F_X^{\text{TPSS}} d\mathbf{r} \quad (9)$$

in which  $\varepsilon_X^{\text{LDA}}$  is the LDA exchange energy density,  $\sigma$  is the spin variable (for  $\alpha$  and  $\beta$  spin, respectively), and  $F_X^{\text{TPSS}}$  is the TPSS enhancement factor

$$F_X^{\text{TPSS}} = 1 + \kappa - \frac{\kappa}{1 + \frac{x}{\kappa}} \quad (10)$$

$\kappa$  is the first functional parameter that is adjusted for PTPSS. The variable  $x$  is given as

$$x = \left\{ \left[ \frac{10}{81} + c \frac{z^2}{(1+z)^2} \right] p + \frac{146}{2025} \tilde{q}_b^2 - \frac{73}{405} \tilde{q}_b \sqrt{\frac{1}{2} \left( \frac{3}{5} z \right)^2 + \frac{1}{2} p^2} + \frac{1}{\kappa} \left( \frac{10}{81} \right)^2 p^2 + 2\sqrt{e} \frac{10}{81} \left( \frac{3}{5} z \right)^2 + e\mu p^3 \right\} / [(1 + \sqrt{e}p)^2] \quad (11)$$

where

$$\begin{aligned} z &= \frac{\tau^{\text{W}}}{\tau} \quad \alpha = \frac{\tau - \tau^{\text{W}}}{\tau^{\text{UEG}}} \\ \tilde{q}_b &= \frac{9}{20} \frac{(\alpha - 1)}{[1 + b\alpha(\alpha - 1)]^{1/2}} + \frac{2p}{3} \\ p &= s^2 = \left( \frac{|\nabla \rho_{\sigma}|}{\rho_{\sigma}^{4/3} 2(3\pi^2)^{1/3}} \right)^2 \end{aligned} \quad (12)$$

$\rho$  is the electron density,  $p$  is the square of the reduced spin variable  $s$ ,  $\tau$  is the kinetic energy density,  $\tau^{\text{W}}$  is the von Weizsäcker kinetic energy density, and  $\tau^{\text{UEG}}$  is the uniform gas kinetic energy density.  $\mu$ ,  $b$ ,  $c$ , and  $e$  are four additional functional parameters that were adjusted for PTPSS.

The TPSS correlation functional is a modification of the correlation part of the Perdew–Kurth–Zupan–Blaha (PKZB) meta-GGA functional<sup>87</sup> and defined as follows

$$E_C^{\text{TPSS}} = \int \rho \varepsilon_C^{\text{revPKZB}} \times \left[ 1 + d \varepsilon_C^{\text{revPKZB}} \left( \frac{\tau^{\text{W}}}{\tau} \right)^3 \right] d^3r \quad (13)$$

with

$$\begin{aligned} \varepsilon_C^{\text{revPKZB}} &= \varepsilon_C^{\text{PBE}}[\rho_{\alpha}, \rho_{\beta}, \nabla \rho_{\alpha}, \nabla \rho_{\beta}] [1 + C(\zeta, \xi) \left( \frac{\tau^{\text{W}}}{\tau} \right)^2] - \\ &\quad [1 + C(\zeta, \xi)] \left( \frac{\tau^{\text{W}}}{\tau} \right)^2 \sum_{\sigma} \frac{\rho_{\sigma}}{\rho} \tilde{\varepsilon}_C \end{aligned} \quad (14)$$

and where

$$\begin{aligned} \tilde{\varepsilon}_C &= \max[\varepsilon_C^{\text{PBE}}[\rho_{\sigma}, 0, \nabla \rho_{\sigma}, 0], \varepsilon_C^{\text{PBE}}[\rho_{\alpha}, \rho_{\beta}, \nabla \rho_{\alpha}, \nabla \rho_{\beta}]] \\ C(\zeta, \xi) &= \frac{0.53 + 0.87\zeta^2 + 0.50\zeta^4 + 2.26\zeta^6}{\left[ 1 + \xi^2 \frac{(1 + \xi)^{-4/3} + (1 - \xi)^{-4/3}}{2} \right]^4} \\ \xi &= \frac{|\nabla \zeta|}{2(3\pi^2 \rho)^{1/3}} \end{aligned} \quad (15)$$

Here,  $\zeta = (\rho_{\alpha} - \rho_{\beta})/\rho$  is the relative spin polarization. The TPSS correlation part depends on two parameters. These are  $d$ , as given in eq 13, and  $\beta$ , which is part of the PBE correlation functional<sup>88</sup>  $\varepsilon_C^{\text{PBE}}$  and the modified  $\tilde{\varepsilon}_C$  (ref 86 gives a detailed description of all the necessary variables in the TPSS functional).

The values of the seven parameters of the original TPSS functional are given in Table 4 in comparison with the refitted values of oTPSS. We note in passing that, in 2007, Perdew et al. also published a reparameterized version of TPSS with different values for  $\mu$ ,  $c$ , and  $e$ <sup>89</sup> (for a redesigned version termed revTPSS, see ref 90).

The fourth major difference between PTPSS and most of the preceding DHDFs regards the fitting procedure. Like for oTPSS, B97-D,<sup>72</sup> or DSD-BLYP, PTPSS is fitted in combination with an empirical London-dispersion correction. Here, we applied the new DFT-D3 scheme.

The fitting procedure was carried out as follows: First of all, the amount of Fock-exchange was set to  $a_X = 0.5$  and kept constant. We regard this value as a reasonable compromise for both main group and transition metal chemistry. We think that a too high fraction of Fock-exchange (e.g., 69% or about 80%, as in DSD-BLYP and XYG3, respectively) makes any DHDF unstable in electronically complicated situations. Evidence for this was already provided for the B2KPLYP functional in ref 15. The seven TPSS parameters and the SOS-PT2 parameter  $a_C$  were fitted in a standard least-squares procedure. The fit set (dubbed DFT fit set)<sup>35</sup> is a modified version of the one we already used for oTPSS. It is comprised of a total of 112 energies. These are 49 atomization energies (47 of the G2/97 set and additionally the adamantane and anthracene molecules, which are of a similar size but whose uniformly accurate description is difficult to achieve with DFs), five total atomic energies, eight atomic ionization potentials, and seven atomic electron affinities (taken from the G2-1 set), six noncovalently bound systems from the S22 set, the (H<sub>2</sub>O)<sub>6</sub> cyclic cluster taken from WATER27, four rare gas dimers from RG6, and 29 decomposition energies from the MB08-165 benchmark set. Furthermore, the isomerization reaction from iso- to *n*-octane, the Diels–Alder reaction between furane and maleic anhydride to form the *endo* product, and the decomposition of Li<sub>8</sub> into lithium dimers (from ALK6) were included. The systems were weighted with different factors for the statistical analysis. The full set and the weight factors are listed in Table S2 in the Supporting Information.

During the fitting procedure, the DFT-D3 parameters were also adjusted. In a prescreening process, we used an  $s_6$  value of 0.5. Later, we readjusted it, as described in section 3.1. The resulting value is 0.75, which is expected, as the functional contains less perturbative correlation than others,



**Table 4.** Parameters of the TPSS,<sup>86</sup> oTPSS,<sup>34</sup> and PTPSS Methods

	<i>b</i>	<i>c</i>	<i>e</i>	$\mu$	$\kappa$	$\beta$	<i>d</i>	<i>a<sub>x</sub></i>	<i>a<sub>c</sub></i>
TPSS	0.40	1.59096	1.537	0.21952	0.804	0.06672	2.8		
oTPSS	3.43	0.75896	0.165	0.41567	0.778	0.08861	0.7		
PTPSS	0.15	0.88491	0.047	0.16952	0.872	0.06080	6.3	0.50	0.375

**Table 5.** Parameters of the PW,<sup>91</sup> mPW,<sup>94</sup> B95,<sup>92</sup> PW6B95,<sup>93</sup> and PWPB95 Methods

	<i>b<sub>PW</sub></i>	<i>c<sub>PW</sub></i>	<i>d<sub>PW</sub></i>	<i>c<sub>opp</sub></i>	<i>c<sub>σσ</sub></i>	<i>a<sub>x</sub></i>	<i>a<sub>c</sub></i>
PW	0.0042	1.6455	4				
mPW	0.00426	1.6455	3.72				
B95				0.0031	0.038		
PW6B95	0.00538	1.7382	3.8901	0.00262	0.03668	0.28	
PWPB95	0.00444	0.3262	3.7868	0.00250	0.03241	0.50	0.269

due to the neglect of the same spin part. The  $s_{r,6}$  and  $s_8$  parameters were determined as described in the DFT-D3 paper (least-squares fit of a special van-der-Waals (vdW) fit set). Technically, we performed some fitting cycles for the electronic PTPSS parameters, then adjusted the DFT-D3 parameters and repeated this several times. The finally obtained parameter values are given in Tables 3 and 4. For these values, PTPSS-D3 yielded a root-mean-square deviation (RMSD) of 3.1 kcal/mol for the DFT fit set and 0.50 kcal/mol for the vdW fit set. More information about results for subsets of the vdW set are shown on our Web site.<sup>51</sup> Compared to TPSS and oTPSS, the parameters significantly change. Also, there are no obvious trends seen when comparing TPSS to oTPSS and TPSS to PTPSS. Particularly, the parameters *b* and *e* become very small, whereas *d* shows a large increase. The SOS-PT2 contribution in PTPSS is  $a_c = 0.375$ .

**3.5. The PWPB95 Functional.** A second new DHDF approach is dubbed PWPB95-D3. It is based on the Perdew–Wang (PW) GGA-exchange<sup>91</sup> and the Becke95 (B95) meta-GGA-correlation<sup>92</sup> functionals (inspired by Zhao and Truhlar’s PW6B95 hybrid-meta-GGA<sup>93</sup>). PW exchange ( $E_X^{PW}$ ) contains three adjustable parameters  $b_{PW}$ ,  $c_{PW}$ , and  $d_{PW}$ .

$$E_X^{PW} = E_X^{LDA} - \sum_{\sigma} \int \rho_{\sigma}^{4/3} \frac{b_{PW}x_{\sigma}^2 - (b_{PW} - \beta)x_{\sigma}^2 \exp(-c_{PW}x_{\sigma}^2) - 10^{-6}x_{\sigma}^{d_{PW}}}{1 + 6b_{PW}x_{\sigma} \sin h^{-1}x_{\sigma} - \frac{10^{-6}x_{\sigma}^{d_{PW}}}{A_x}} d^3r \quad (16)$$

with

$$x_{\sigma} = \frac{|\nabla \rho_{\sigma}|}{\rho_{\sigma}^{4/3}}, \quad \beta = 5(36\pi)^{-5/3}, \quad A_x = -\frac{3}{2} \left( \frac{3}{4\pi} \right)^{1/3} \quad (17)$$

The original parameter values for PW, the modified mPW,<sup>94</sup> and the reparameterized PW6B95 functional are shown in Table 5.

The B95 correlation functional can be divided into one part treating electron pairs of opposite spin ( $E_C^{pp}$ ) and another one for those of same spin ( $E_C^{\sigma\sigma}$ ):

$$E_C^{B95} = E_C^{B95,opp} + \sum_{\sigma} E_C^{B95,\sigma\sigma} \quad (18)$$

with

$$E_C^{B95,opp} = \frac{E_C^{PW}(\rho_{\alpha}, \rho_{\beta}) - E_C^{PW}(\rho_{\alpha}, 0) - E_C^{PW}(0, \rho_{\beta})}{(1 + c_{opp} \sum_{\sigma} x_{\sigma}^2)} \quad (19)$$

$$E_C^{B95,\sigma\sigma} = \frac{2(\tau_{\sigma} - \tau_{\sigma}^W)E_C^{PW}(\rho_{\sigma}, 0)}{\frac{3}{5}(6\pi^2)^{2/3} \rho_{\sigma}^{5/3} (1 + c_{\sigma\sigma} x_{\sigma}^2)^2} \quad (20)$$

where  $E_C^{PW}$  is Perdew and Wang’s correlation LSDA functional.<sup>95</sup> B95 correlation depends on two adjustable parameters  $c_{opp}$  and  $c_{\sigma\sigma}$ . The original B95 and the reparameterized PW6B95 values are also shown in Table 5.

Similar as in PTPSS-D3, the inherent functional parameters were refitted for PWPB95. PWPB95 also includes an SOS-PT2 correlation term. Due to the fact that B95 differs between a same and an opposite spin contribution, two different approaches for the PWPB95 functional are possible.

In the first one, the entire reparameterized B95 functional is scaled down by  $1 - a_c$ , where  $a_c$  is the scale parameter for the opposite spin perturbative contribution:

$$E_{XC}^{PWPB95} = (1 - a_x)E_X^{PW} + a_x E_X^{HF} + (1 - a_c)E_C^{B95} + a_c E_C^{OS-PT2} \quad (21)$$

This approach is in complete analogy with the PTPSS functional.

A second possibility is to include 100% of reparameterized, same-spin B95 correlation and to just scale down the opposite spin part by  $1 - a_c$ :

$$E_{XC}^{PWPB95} = (1 - a_x)E_X^{PW} + a_x E_X^{HF} + \sum_{\sigma} E_C^{B95,\sigma\sigma} + (1 - a_c)E_C^{B95,opp} + a_c E_C^{OS-PT2} \quad (22)$$

We considered both approaches and thoroughly compared them with each other. Our findings showed that the first approach yielded much better results for GMTKN30 than the second one. Thus, we will from now on refer to eq 21 whenever we discuss PWPB95.

PWPB95-D3 contains two adjustable parameters less than PTPSS-D3. Preliminary tests made it necessary to modify the fitting procedure compared to PTPSS-D3. Only one fit set was used with higher weights on noncovalently bound complexes. The DFT-D3 parameters ( $s_{r,6}$ ,  $s_8$ ) were fitted at the same time as the five functional parameters and the scale parameter  $a_c$ . Details about the fit set can be found in Table S3 of the Supporting Information. The amount of Fock-exchange was also fixed to 50%. The resulting RMSD value is 2.6 kcal/mol for the fit set compared to 3.6 kcal/mol for the alternative PWPB95-D3 approach according to eq 22. The finally obtained parameter values are given in Tables 3

and 5. All DFT parameters are smaller than for PW6B95. The parameter  $b_{\text{PW}}$  is significantly smaller than for all other functionals based on PW exchange (note that this was also observed for the reparameterized oPWLYP GGA-functional in ref 35). The SOS-PT2 contribution is, with  $a_{\text{C}} = 0.269$ , smaller than for PTPSS-D3. The  $s_6$  value was adjusted as for the other DHDFs and is, as expected, larger than for PTPSS-D3 ( $s_6 = 0.82$ ).

## 4. Computational Details

All calculations were carried out with a modified version of TURBOMOLE 5.9 and the original version of TURBOMOLE 6.0.<sup>96–99</sup> For the GMTKN30 analysis and the fitting procedures, the large Ahlrichs' type quadruple- $\zeta$  basis sets def2-QZVP were applied,<sup>100</sup> which yield results quite close to the Kohn–Sham limit. For the calculations of electron affinities, diffuse s and p functions (for hydrogen, only an s function) were added from the Dunning aug-cc-pVQZ basis sets;<sup>79</sup> the resulting set is denoted by aug-def2-QZVP. As discussed previously,<sup>35</sup> one diffuse s and one diffuse p function (taken from aug-cc-pVQZ) was added to oxygen in the case of WATER27. We also carried out calculations for GMTKN30 with the def2-TZVPP set and used diffuse functions from aug-cc-pVTZ where necessary. To account for scalar relativistic effects, the heavy atoms in HEAVY28 and RG6 were treated with the effective core potentials ECP-28 (for Sb–Xe) and ECP-60 (for Pb, Bi, and Rn),<sup>101,102</sup> which were slightly modified by Weigend and Ahlrichs and called “def2-ecp” in Turbomole.<sup>100</sup>

For all hybrid-(meta-)GGA parts of the DHDFs and for general hybrid functionals, the resolution of the identity (RI-JK) approximation was applied.<sup>103</sup> For the perturbative parts of the DHDFs, the RI approximation was used as well.<sup>99</sup> Auxiliary basis functions were taken from the TURBOMOLE basis set library.<sup>104,105</sup> In all cases, SCF convergence criteria were set to  $10^{-7} E_h$ . For GMTKN30 calculations, the TURBOMOLE grid  $m4$  was used, whereas the larger  $m5$  grid was chosen in the fitting procedure.<sup>105</sup> All open-shell calculations were done within the unrestricted Kohn–Sham formalism (UKS). The study of GMTKN30 was carried out with the DHDFs B2PLYP,<sup>7</sup> B2GPPLYP,<sup>15</sup> DSD-BLYP,<sup>20</sup> XYG3,<sup>21</sup> PTPSS, and PWPB95 and as a comparison with the hybrids B3LYP<sup>106,107</sup> and PW6B95.<sup>93</sup> In all cases except for XYG3, the new empirical London dispersion correction (DFT-D3)<sup>43</sup> was applied, for which a separate program was used, which is available for download from our Web site.<sup>51</sup>

The study of dissociation reactions of transition metal carbonyls is based on a publication by Hyla-Kryspin and Grimme.<sup>108</sup> To make our evaluation consistent with this previous publication, we followed the same technical procedures. All calculations were carried out with a triple- $\zeta$  Gaussian basis augmented with polarization functions: (17s11p6d1f)/[6s4p3d1] for the transition metal and (11s6p2d)/[5s3p2d] for C and O.<sup>109</sup> Geometry optimizations were carried out with the BP86 functional.<sup>73,110</sup> Reaction enthalpies for the dissociation reactions (for more details, see section 5.25) were calculated as

$$\Delta H_R^{298} = \Delta E_{\text{elec}} + \Delta \text{ZPVE} + \Delta H_{0 \rightarrow 298} + \Delta(PV) \quad (23)$$

where  $E_{\text{elec}}$  is the electronic energy, ZPVE is the zero point vibrational energy,  $H_{0 \rightarrow 298}$  is the thermal correction for a temperature of 298.15 K, and  $\Delta(PV)$  is the (ideal gas) volume work.  $\Delta \text{ZPVE}$  and  $\Delta H_{0 \rightarrow 298}$  were calculated with the BP86 functional by using the SNF<sup>111</sup> program and applied for all tested functionals.

## 5. Results and Discussion

**5.1. The GMTKN30 Database.** *5.1.1. Results for (aug-)def2-QZVP.* The MADs and RMSDs for all functionals obtained with (aug-)def2-QZVP are shown in Tables S4–S11 in the Supporting Information. As both values provide the same conclusions, only MADs will be discussed in the following. First of all, the DHDFs are compared with functionals on the hybrid level. In our study, these are the B3LYP-D3 and PW6B95-D3 methods. We note in passing that the latter clearly outperforms B3LYP-D3 and is, according to our experience, overall one of the best hybrid functionals on the market.

The graphs in Figure 2 show the ratios between the MADs of the double-hybrids and the hybrids. This comparison confirms that all DHDFs outperform the hybrids. The only exceptions are the noncovalent interactions, for which B3LYP-D3 is significantly better than XYG3 for S22, ADIM6, RG6 (factor of 3), HEAVY28, PCONF, and ACONF. PTPSS-D3 is slightly worse than B3LYP-D3 for RG6, PCONF, and ACONF. B3LYP-D3 is better than PWPB95-D3 for HEAVY28. However, in these last four cases, the PTPSS-D3, PWPB95-D3, and B3LYP-D3 methods are already within the errors of the reference values, and thus, this comparison should be interpreted with care. The comparison between the DHDFs and PW6B95-D3 shows again that PW6B95-D3 is outperformed in most of the cases but that the ratios are closer to unity and in a narrower range than for B3LYP-D3. PW6B95-D3 is, like B3LYP-D3, better than XYG3 for noncovalent interactions. The high ratios for the RG6 set, though, are a bit misleading, as all DHDFs, except XYG3, yield excellent MADs for that set: 0.06 (B2PLYP-D3), 0.05 (B2GPPLYP-D3), 0.07 (DSD-BLYP-D3), 0.09 (PTPSS-D3), 0.05 (PWPB95-D3), and 0.20 kcal/mol (XYG3) compared to 0.03 kcal/mol (PW6B95-D3).

After having seen that mixing in a perturbative correlation generally improves the results compared to fourth-rung functionals, we concentrate now on a comparison of the results for the DHDFs. All MADs based on (aug-)def2-QZVP calculations can be found in the left column of Figure 3. The MB08-165 set contains very difficult, randomly created molecular systems and is a very good indicator for the robustness of a quantum chemical method. B2PLYP-D3, B2GPPLYP-D3, and PTPSS-D3 are in a same range, with MADs of about 4 kcal/mol. XYG3 is significantly worse, with 5.2 kcal/mol (even the PW6B95-D3 hybrid is better with 4.7 kcal/mol). DSD-BLYP-D3 is a clear improvement, with 3.4 kcal/mol. PWPB95-D3 yields the best MAD ever reported for this test set (2.5 kcal/mol). This value is in the range of CCSD(T)/cc-pVQZ, that was reported to yield an MAD of 2.6 kcal/mol.<sup>32</sup> This finding can be

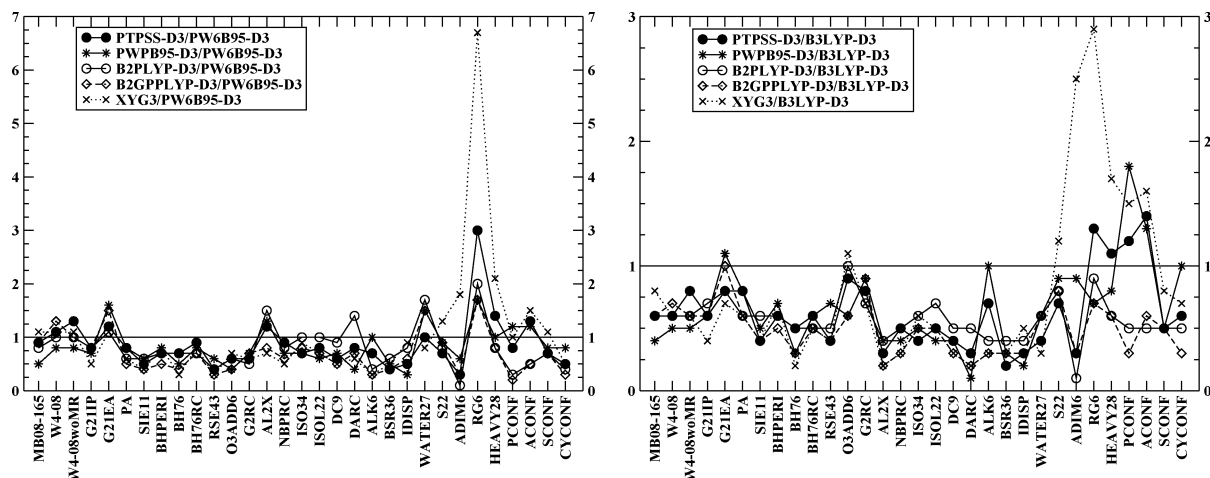


**Figure 2.** Ratios of the MADs of different functionals: comparisons between the DHDFs and PW6B95-D3 (left); comparisons between the DHDFs and B3LYP-D3 (right). All calculations were carried out with (aug)-def2-QZVP. To make the curves better distinguishable from each other, the curves for the DSD-BLYP functional were left out. The results are in qualitative agreement with those shown in the figures, though.

interpreted as a first hint on the robustness of this functional. PWPB95-D3 also gives the best MAD for the atomization energy test set (1.9 kcal/mol). The other five DHDFs are within a range of 2.4–3.0 kcal/mol and quite similar to each other. This similarity is in contrast to frequent claims in favor of XYG3 over B2PLYP, which are based on the calculations of HOFs.<sup>41</sup> Because theoretical HOFs are basically atomization energies, this discrepancy is at present not understandable for us. For ionization potentials, XYG3 yields the best MAD (1.4 kcal/mol), whereas the other DHDFs are in the range of about 2.0–2.3 kcal/mol. Electron affinities are almost equally well described by XYG3, B2PLYP-D3, and PTPSS-D3, whereas the description is slightly worse for B2GPPLYP-D3, DSD-BLYP-D3, and PWPB95-D3. A similar trend can also be seen for proton affinities, with the exception that PTPSS-D3 and PWPB95-D3 are slightly worse than the other four methods (note that here delocalized systems also play a role and that the delocalization error is expected to be larger the less Fock-exchange is included).

Larger differences in the MADs are observed for SIE-related problems. The SIE11 set is best described by XYG3 and DSD-BLYP-D3, with 3.1 kcal/mol, followed closely by B2GPPLYP-D3, with 3.4 kcal/mol. B2PLYP-D3 shows the worst MAD of the DHDFs, with 4.9 kcal/mol. This trend follows qualitatively the amount of Fock-exchange that decreases when going from XYG3 to DSD-BLYP, to B2GPPLYP, and to B2PLYP. However, PTPSS-D3 and PWPB95-D3 have the lowest amount of Fock-exchange of all DHDFs, and their MADs are, with 3.9 and 4.3 kcal/mol, better than for B2PLYP-D3. A possible explanation might be the single-electron SIE correction within the TPSS and B95 parts. The result for the barrier heights of the substitution, association, and unimolecular and transfer reactions within BH76 shows a slightly different picture. Here, XYG3, DSD-BLYP-D3, and B2GPPLYP-D3 are the best functionals with MADs of 1.1, 1.2, and 1.3 kcal/mol. This time, though, B2PLYP-D3 and PTPSS-D3 have the same MADs, with 2.5 kcal/mol. PWPB95-D3 gives 1.8 kcal/mol. However, this picture cannot be generalized to other barriers, particularly when larger (closed-shell) systems are involved. This is seen

from the results for BHPERI, where XYG3 and PWPB95-D3 are the worst functionals, with 1.9 kcal/mol, followed by PTPSS-D3, with 1.7 kcal/mol, by B2PLYP-D3 (1.6 kcal/mol), by B2GPPLYP-D3 (1.3 kcal/mol), and by DSD-BLYP-D3 (1.2 kcal/mol).

The evaluation of reaction energies shows a heterogeneous picture, however, at a generally high level of accuracy. In some cases, the MADs of all six functionals are close to each other (e.g., for BH76RC), and in other cases, they differ significantly (for O3ADD6, AL2X, ISOL22, DC9, DARC, ALK6, and BSR36). However, no single DHDF is consistently the best one. XYG3 is the best functional in the case of AL2X and together with DSD-BLYP-D3 for NBPIC. DSD-BLYP-D3 is, moreover, the best method for DC9 and BSR36. B2GPPLYP-D3, PTPSS-D3, and PWPB95-D3 results are often very close, though. Sometimes, XYG3 can be also the worst functional, and it is comparable to B2PLYP-D3. The new PTPSS-D3 performs best for ISO34 (MAD = 0.9 kcal/mol). PWPB95-D3 is the best functional for O3ADD6 (1.7 kcal/mol, together with B2GPPLYP-D3), ISOL22 (2.9 kcal/mol), and DARC (1.5 kcal/mol). However, it has an outlier for ALK6 (4.6 kcal/mol), which is almost the same value as for B3LYP-D3 and PW6B95-D3 (4.7 kcal/mol).

The results for the noncovalent interactions test sets are more uniform. Intramolecular dispersion interactions within IDISP are best described by PWPB95-D3 (MAD = 1.2 kcal/mol), followed by DSD-BLYP-D3 (MAD = 1.4 kcal/mol), PTPSS-D3 (MAD = 1.7 kcal/mol), and B2GPPLYP-D3 (2.1 kcal/mol). B2PLYP-D3 and XYG3 have larger MADs with 3.0 and 3.1 kcal/mol. The water clusters in WATER27 are best described by XYG3, DSD-BLYP-D3, and PTPSS-D3 with 1.4, 1.5, and 1.6 kcal/mol. PWPB95-D3, B2GPPLYP-D3 and B2PLYP-D3 have MADs of 2.4, 2.6, and 2.8 kcal/mol. The S22 set is best described by PTPSS-D3 with a very low MAD of 0.25 kcal/mol. It is followed by B2PLYP-D3 (0.27 kcal/mol), DSD-BLYP-D3 (0.28 kcal/mol), B2GPPLYP-D3 (0.30 kcal/mol), PWPB95-D3 (0.32 kcal/mol), and XYG3 (0.45 kcal/mol). Note that we did not use any London-dispersion correction for XYG3, as in recent publications it



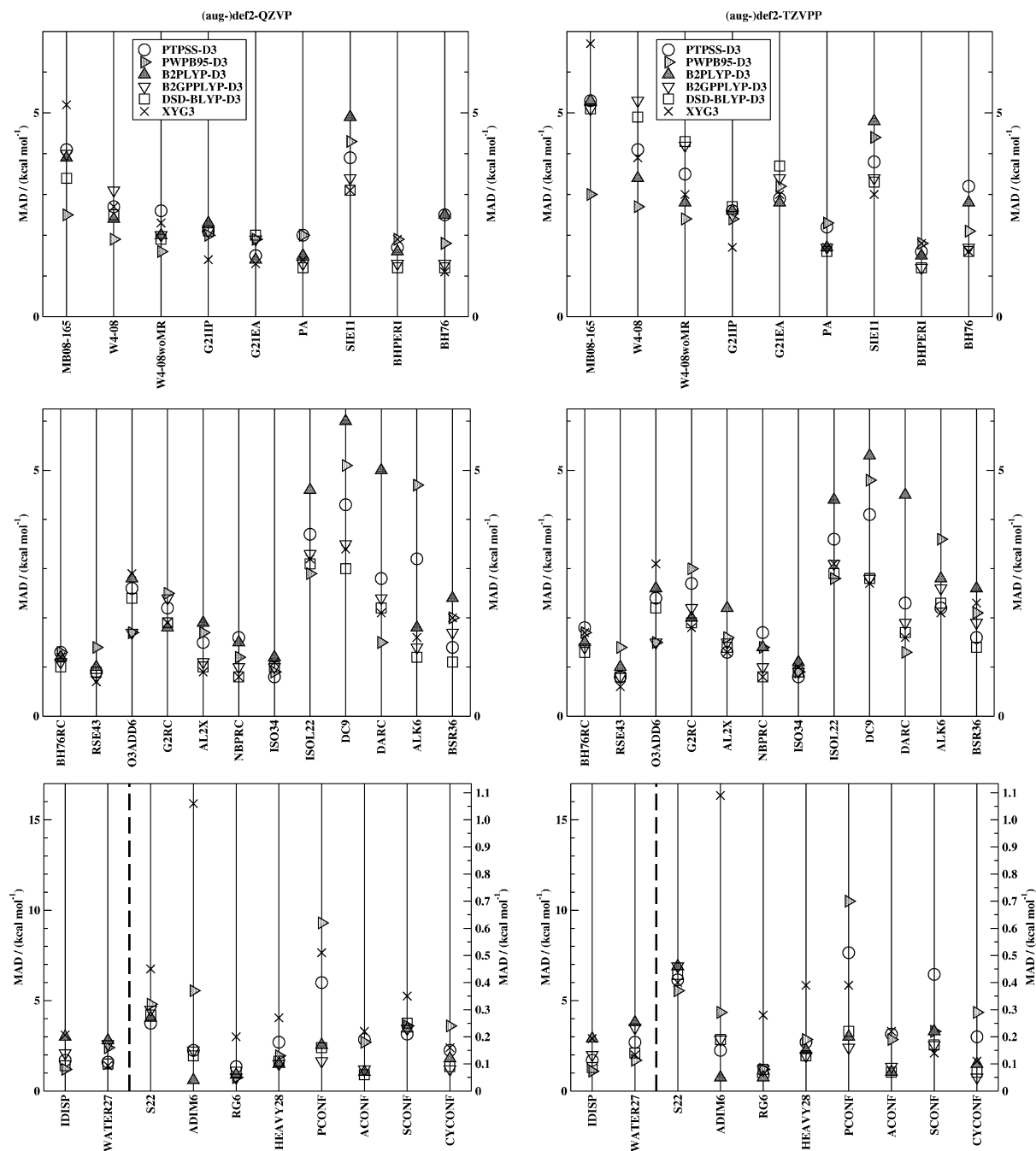


**Figure 3.** MADs for PTPSS-D3, PWPB95-D3, B2PLYP-D3, B2GPPLYP-D3, DSD-BLYP-D3, and XYG3 in kcal/mol for the complete GMTKN30 database with (aug-)def2-QZVP (left column) and (aug-)def2-TZVPP (right column). For the sets to the right of the dashed lines, the right MAD axes apply.

was argued that XYG3 works also very well for dispersion dominated interactions on its own.<sup>21–23,50,85</sup> Indeed, the overall behavior is not bad at first glance, but the comparison with the results for the other functionals shows that dispersion interactions are not fully considered in XYG3. A very prominent example is the ADIM6 test set, for which XYG3 yields a large MAD of 1.1 kcal/mol, whereas the other MADs are <0.15 kcal/mol, which is within the accuracy of the reference method (except for PWPB95-D3, with 0.36 kcal/mol). Also, for the other subsets (except for PCONF, where PTPSS-D3 and PWPB95-D3 have MADs of 0.40 and 0.62 kcal/mol), it can be seen that all DHDFs, except XYG3, are close to the accuracy of the estimated CCSD(T)/CBS

reference values. Therefore, a direct comparison between these five functionals and a ranking of them is not appropriate. Dispersion corrections for XYG3 in its present form make no sense because double-counting effects cannot be avoided for such a highly nonlocal functional that has been parametrized without such corrections.

To better rationalize the results discussed above, one can simply count how many times a certain DHDF yields the best MAD or RMSD for a subset. The results are depicted in Figure 4. B2PLYP-D3 yields the best MAD in three, B2GPPLYP-D3 in five, DSD-BLYP-D3 in nine, XYG3 in eight, PTPSS-D3 in three, and PWPB95-D3 in seven cases. This picture allows a conclusion that strongly favors the

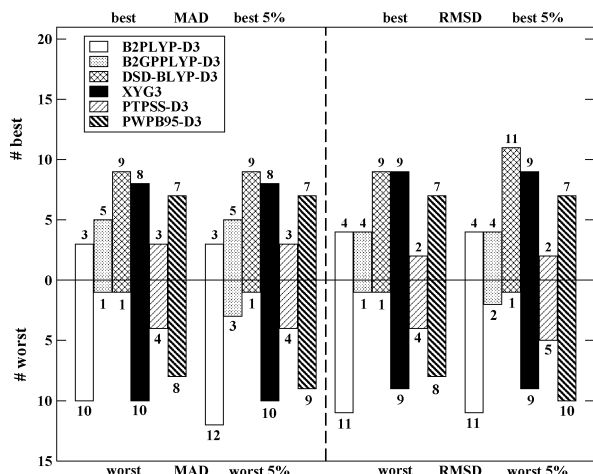


**Figure 4.** Analysis of how many times a certain double-hybrid yields the best and the worst MAD (left) or RMSD (right) for all subsets of GMTKN30 and how many times a functional is within a 5% range of the best/worst MAD or RMSD.

DSD-BLYP-D3 and XYG3 functionals. However, if one also counts how many times a certain DHDF is the worst compared to the other DHDFs, one obtains a different picture. B2PLYP-D3 and XYG3 yield the worst MADs in 10 cases each. PWPB95-D3 follows with eight cases. PTPSS-D3 is the worst functional in only four cases, B2GPPLYP-D3 and DSD-BLYP-D3 in one case each. Thus, on the one hand, XYG3 seems to compete with the DSD-BLYP-D3 method, but on the other hand, it is also by far outperformed by DSD-BLYP-D3, B2GPPLYP-D3, and PTPSS-D3 and as bad as B2PLYP-D3. PWPB95-D3 shows a similar trend but is slightly better than XYG3 in this analysis. We think that, besides always obtaining the best MAD for a certain subset, it is also important that a functional is robust and shows a uniform accuracy for a whole range of different properties. Testing for robustness is the main reason why we created the GMTKN24/30 databases. Particularly, when being challenged by new chemical problems, it is in our opinion wiser to use a functional that is more robust. The results shown in Figure 4 give a hint on this property. The RMSDs on the right-hand side of Figure 4 allow the same conclusions. Besides just counting how many times the best or the worst MAD/RMSD is obtained, we also analyzed how many times a functional is within a 5% range of the best and worst result. These trends are comparable to the ones discussed above.

A third statistical evaluation of the results is carried out by considering the WTMADs (Figure 5). All six double hybrids have lower WTMADs than PW6B95-D3, the best hybrid. Again, we observe that the London-dispersion correction improves the results. B2PLYP-D3 has a WTMAD of 2.0 kcal/mol, which is the worst, compared to the other DHDFs. XYG3 is, by 0.1 kcal/mol, better (WTMAD = 1.9 kcal/mol). PTPSS-D3 yields the same WTMAD. B2GPPLYP-D3 is, with 1.7 kcal/mol, the third best; PWPB95-D3, with 1.6 kcal/mol, the second best; and DSD-BLYP-D3, with 1.5 kcal/mol, the best DHDF. This again indicates the better overall performance of DSD-BLYP-D3 and PWPB95-D3. The new PWPB95-D3 functional is thus a significant improvement over B2PLYP, XYG3 and B2GPPLYP and a

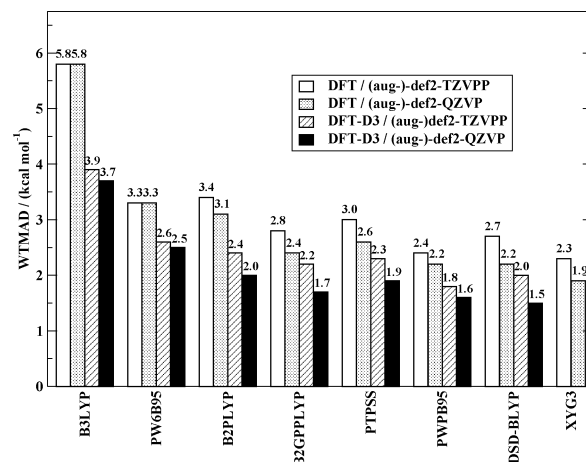


**Figure 5.** Weighted total mean absolute deviations (WTMADs) in kcal/mol for all tested methods with and without dispersion correction. The values are based on (aug-)def2-TZVPP and (aug-)def2-QZVP calculations.

good alternative to DSD-BLYP-D3, at a much lower computational cost for large systems and employing less nonlocality.

**5.1.2. Basis Set Dependence.** In section 3, it was discussed that the different DHDFs were developed by applying basis sets of different quality. The basis set dependences of the Fock-exchange and perturbative correlation parameters were already studied.<sup>14,15,18</sup> Furthermore, also, a justified question was raised as to whether a functional fitted with a triple- $\zeta$  basis set works better in practice with a basis set of similar quality than a functional developed with a quadruple- $\zeta$  basis.<sup>21–23,50</sup> This is particularly important, as in common applications, basis sets of quadruple- $\zeta$  quality, as used here, are not always feasible.

The GMTKN30 database allows us to answer this question on very solid ground. The right column of Figure 3 shows the MADs of all 30 subsets obtained with the (aug-)def2-TZVPP basis (see also Tables S12–S19, Supporting Information). Figure 5 shows the WTMADs with and without dispersion correction for all tested methods. It can be seen that the basis set effect for the hybrid functionals is very small. The WTMADs increase by merely 0.2 and 0.1 kcal/mol for B3LYP-D3 and PW6B95-D3 (to 3.9 and 2.6 kcal/mol), and we can conclude that for these functionals the Kohn–Sham limit is almost reached with the (aug-)def2-TZVPP basis. The basis set dependence for most of the DHDFs is stronger, though. Usually, the MADs for the subsets worsen; sometimes they become slightly better. The stronger effect can be explained by the presence of the WF-based perturbative correction. Interestingly, DSD-BLYP-D3 and B2GPPLYP-D3 results lie closer to each other than on the quadruple- $\zeta$  level. This can, for example, be seen for MB08-165, where both functionals yield the same MADs of 5.1 kcal/mol.

The WTMADs of B2PLYP-D3 and XYG3 worsen by 0.4 kcal/mol compared to the quadruple- $\zeta$  level. B2GPPLYP-D3 and DSD-BLYP-D3 are even more affected (increase of 0.5 kcal/mol), which is in line with their large PT2 contributions. PTPSS-D3 gets worse by 0.4 kcal/mol. PWPB95-D3 shows the least basis set dependence (increase from 1.6 to

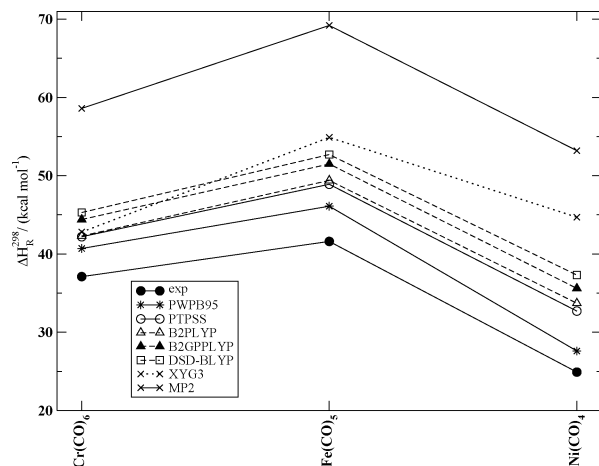


**Figure 6.** Reaction enthalpies ( $\Delta H_R^{298}$ ) in kcal/mol for the first CO dissociation reaction of three transition metal carbonyls. The values were obtained with the PWPB95, PTPSS, B2PLYP, B2GPPLYP, DSD-BLYP, and XYG3 methods. Vibrational and thermal corrections are based on BP86 calculations. A triple- $\zeta$  basis was applied in all cases [(17s11p6d1f)/[6s4p3d1] for the transition metal and (11s6p2d)/[5s3p2d] for C and O]. The experimental and MP2 values are taken from ref 108.

1.8 kcal/mol) and is, thus, the only DF that has a WTMAD below 2 kcal/mol at this basis set level. Thus, at the triple- $\zeta$  level, the order of accuracy changes. B2PLYP-D3 still has the largest WTMAD compared to the other DHDFs (2.4 kcal/mol). XYG3 and PTPSS-D3 have WTMADs of 2.3 kcal/mol and are followed closely by B2GPPLYP-D3 with 2.2 kcal/mol. DSD-BLYP-D3 is the second best method, with 2.0 kcal/mol. PWPB95-D3 is the best method, with 1.8 kcal/mol, although it was fitted with a quadruple- $\zeta$  basis. In fact, this also indicates a higher robustness of PWPB95-D3 compared to the other DHDFs. According to these results, the answer to the question, whether a functional fitted with a triple- $\zeta$  basis set gives relatively better results when applied with such a basis set, is clearly no and thus contrary to claims in the literature.<sup>21–23,50</sup> The WTMADs are just shifted, and the differences between XYG3 and B2PLYP-D3 are still the same compared to the quadruple- $\zeta$  results. Our findings, also contradict recent claims that the basis set dependence of XYG3 is similar to that of B3LYP.<sup>23</sup>

**5.2. Performance for Transition Metal Carbonyls.** In the theoretical section about the DHDFs, we argued, that we have chosen the Fock-exchange parameter to be one-half, so that both, main group and transition metal chemistry, can be described adequately. As a test of this hypothesis, we studied the dissociation of one CO ligand in the  $\text{Cr(CO)}_6$ ,  $\text{Fe(CO)}_5$ , and  $\text{Ni(CO)}_4$  isoelectronic series, which is sensitive to details of the correlation treatment. Reaction enthalpies were calculated as described in the computational details section and are shown in Figure 6. Experimental and MP2 values,<sup>108</sup> which were obtained with the same basis set and the same vibrational and thermal corrections as for the DHDFs, are also given (see also Table S20, Supporting Information).

All theoretical methods overestimate the experimental values. PWPB95, though, is closest to the reference, followed by PTPSS, B2PLYP, B2GPPLYP, DSD-BLYP, XYG3, and

MP2. As anticipated, the amount of Fock-exchange and the size of the error are strongly related. Interestingly, the values for all methods, except for XYG3, are just shifted with respect to the experiment (the connecting lines in Figure 6 are almost parallel to the experimental reference). This, however, is not observed for XYG3, for which the chromium compound is relatively better described than the other two compounds and the dissociation energy of  $\text{Ni(CO)}_4$  is incorrectly computed to be higher than for  $\text{Cr(CO)}_6$ .

**5.3. A Comment on the XYG3 Functional.** We have discussed many results for main group chemistry and given some insight into the functionals' performance for an exemplary transition metal reaction. We concluded that PWPB95 and PTPSS seem to be rather robust functionals and that also XYG3 seems to perform reasonably well, yielding good MADs in many cases. In this section, we further want to comment on XYG3 and give a new explanation for its good performance.

In their original XYG3 paper, the authors argue that the hybrid-GGA part of B2PLYP (i.e., B2LYP) does not employ 100% of DFT correlation and that this "truncated DFT" method yields densities and orbitals "that are dramatically different from the real ones." They argue that using B3LYP densities and orbitals for the evaluation of XYG3 is the key ingredient for the functional's good performance, because B3LYP densities had been shown to be "similar to those from CCSD(T) wave functions" and because B3LYP has 100% DFT correlation.

We do not agree with this interpretation. Of course, e.g., for thermochemical properties, some correlation is missing in B2LYP. This can be seen, when, e.g., the WTMADs for the GMTKN30 set for B3LYP<sup>112</sup> and B2LYP are compared with each other (6.7 vs 9.4 kcal/mol). However, the missing 27% LYP correlation does not affect significantly either the shape of the orbitals or the electron density. On the contrary, the results for electronic excited states (vertical excitation energies, oscillator and rotational strengths) are practically the same for TD-B2LYP and TD-B3LYP, as discussed by us several times.<sup>36–38</sup> The reason for this is the comparable one-particle spectrum for both methods. B3LYP has the same ingredients as B2LYP, including similar amounts of Fock-exchange, and in principle the two methods just differ by the amounts of LYP correlation. In our context, it is the amount of Fock-exchange that is the decisive factor for the orbital energies. In fact, the occupied part for normal molecules is rather similar for different functionals (and even overlaps to HF are large).<sup>113</sup> The reason for this is the exchange and not the correlation part! In fact, large differences are found for the virtual spectrum, which is worse with B3LYP due to the wrong asymptotic behavior of the larger (compared to B2LYP) GGA part. This can be also seen from theoretical electronic spectra, particularly including excitations into (diffuse) Rydberg orbitals.<sup>114</sup> Thus, we do not think that excitations to B3LYP virtual orbitals lead to better results in a perturbation theory because B3LYP has 100% DFT correlation. Instead, we tentatively assign part of the relatively high accuracy of XYG3 for main group problems to the small amount of Fock-exchange in the orbital generation step, which improves, e.g., spin-contaminated



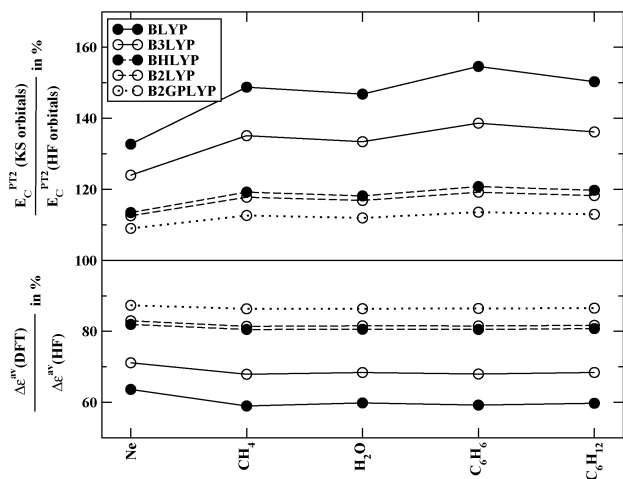


**Figure 7.** Percentage ratios of the averaged orbital energy gap ( $\Delta\epsilon^{av}$ ) of five molecules for different KS-DFT methods and HF theory (lower part) and ratios between unscaled PT2 correlation energies based on KS and HF orbitals (upper part). All calculations were carried out with def2-QZVP.

problems (see also ref 115 for a recent investigation that also compares orbital energies with the amount of Fock-exchange).

In the following, we would like to underline the similarities between BHLYP and B2LYP and would like to support the above statements by solid data. Therefore, we carried out SCF calculations for five examples (Ne, CH<sub>4</sub>, H<sub>2</sub>O, C<sub>6</sub>H<sub>6</sub>, and C<sub>6</sub>H<sub>12</sub>) with BLYP, B3LYP, BHLYP, B2LYP, B2GPPLYP, and HF (def2-QZVP basis). We then calculated an average occupied–virtual orbital gap  $\Delta\epsilon^{av}$  for each method. We created for each system and each method all possible single excitations from the occupied valence orbitals into the corresponding valence virtual orbitals and then took the average over all excitation energies.

The actual energy values can be found in Table S21 (Supporting Information). We then related the  $\Delta\epsilon^{av}(DFT)$  values obtained for the Kohn–Sham methods to  $\Delta\epsilon^{av}(HF)$  obtained at the HF level. This is shown in the lower half of Figure 7. All average DF gaps are smaller than for HF. For each method, this underestimation seems to be rather system-independent. An inverse relation between the amount of Fock-exchange and  $\Delta\epsilon^{av}$  can be seen. BLYP yields only about 60% of the HF gap, and B2GPPLYP gives the highest ratio of 87%. The results for B2LYP and BHLYP are very similar, proving the above statement, that only the amount of Fock-exchange is important for the one-particle spectrum and not the portion of LYP correlation. B3LYP has a lower average gap than B2LYP (68% vs 81%).

Furthermore, we carried out a standard second-order perturbative calculation based on the different KS orbitals and eigenvalues and related the resulting unscaled correlation energies to the canonical MP2 result (top part of Figure 7). As expected, the absolute correlation energies based on KS orbitals are higher than for MP2. The values obtained with BHLYP and B2LYP are very similar. The PT2 correlation energy is found to be inversely proportional to the amount of Fock-exchange as expected from the orbital energy differences entering the denominator of the PT2 energy expression.

As B3LYP yields a lower gap, a PT2 calculation with B3LYP orbitals yields a higher absolute correlation energy than for B2LYP orbitals. Consequently, the XYG3 functional includes a higher amount of “effective” PT2 correlation than B2LYP and B2GPPLYP. This can be quantified by scaling the actual parameters  $a_C$  (which are 0.27, 0.36, and 0.3211 for the three functionals) by the average factor by which the MP2 correlation is overestimated, i.e., 1.169 for B2PLYP, 1.120 for B2GPPLYP, and 1.335 for XYG3 (Figure 7). These “effective” PT2 contributions are 32% for B2PLYP, 40% for B2GPPLYP, and 43% for XYG3. Thus, part of the explanation for the good behavior of XYG3 is not the fact that B3LYP orbitals are “better” than B2LYP ones due to 100% DFT correlation but that a PT2 treatment with B3LYP orbitals introduces an effectively higher amount of nonlocal correlation.

Furthermore, compared to the B2PLYP and B2GPPLYP, XYG3 has a very reduced amount of repulsive gradient corrected exchange contribution ( $\Delta E_X^{B88}$ ). This, in combination with the higher effective nonlocality, explains why in some studies on noncovalent interactions XYG3 yielded reasonable results.<sup>21,22,50,85</sup> Note, however, that this only holds for small- and medium-sized complexes as XYG3 misses asymptotically about 57% of the dispersion energy due to an effective  $a_C$  of 0.43.

Although decoupling the orbital/density generation and the actual functional evaluation seems to give reasonable results for ground state related problems, we are not sure whether this argument also holds for other properties. A time-dependent treatment of excited states within a TD-XYG3 formalism, for example, would lead to a not well-defined RPA-type matrix because of the different treatments of orbital energies and the functional’s kernel. This is not the case for TD-B2PLYP and TD-B2GPPLYP.<sup>36,38</sup>

## 6. Conclusions

We presented an extension and modification of the recently published GMTKN24 database<sup>35</sup> for applications to general main group thermochemistry, kinetics, and noncovalent interactions. This extended and improved version is called GMTKN30 and comprises 30 different benchmark sets. In total, 1218 single point calculations have to be carried out to evaluate 841 data points (relative energies). In this study, we particularly focused on the analysis of double-hybrid density functionals (DHDFs) and presented two new DHDFs called PTPSS and PWPB95. PTPSS consists of semilocal TPSS exchange and correlation parts, for which seven inherent functional parameters were refitted. PWPB95 contains reparameterized PW exchange and B95 parts (five parameters). Both functionals mix in 50% of nonlocal Fock-exchange, which is less than for other DHDFs. PTPSS includes 37.5% and PWPB95 includes 26.9% of spin-opposite scaled second-order perturbative correlation (SOS-PT2). When combined with a Laplace transformation type algorithm, they scale only as  $O(N^4)$  with system size. Furthermore, both methods are combined with the latest version of the empirical London-dispersion correction (DFT-D3),<sup>43</sup> for which we also presented a new scheme with which to estimate a DHDF’s  $s_6$  scaling parameter. PTPSS-D3 and

PWPB95-D3 were studied for the complete GMTKN30 database and dissociation reactions of three prototypical transition metal carbonyls. The results were compared with the hybrids B3LYP and PW6B95 and with the double hybrids B2PLYP, B2GPPLYP, DSD-BLYP, and XYG3. The analyses led to the following conclusions:

- (1) All double hybrids clearly outperform the hybrid functionals. B2PLYP-D3, B2GPPLYP-D3, and PTPSS-D3 yield very good MADs (about 4 kcal/mol) for the difficult MB08-165 subset, for which XYG3 is even worse than the hybrid PW6B95-D3. DSD-BLYP-D3 is better with 3.4 kcal/mol. PWPB95-D3 yields an excellent result of 2.5 kcal/mol, which is better than CCSD(T)/cc-pVQZ results (2.6 kcal/mol). XYG3 is also worse for noncovalent interactions than the other dispersion-corrected DHDFs, and the errors can reach up to 1 kcal/mol (MAD for alkane dimers). The other five methods usually have errors, which are already within the accuracy of the respective reference data (MADs of less than about 0.2 kcal/mol). Over the whole GMTKN30 database, DSD-BLYP-D3 yields in nine cases the best MAD compared with the other double hybrids (eight for XYG3, seven for PWPB95-D3, five for B2GPPLYP-D3, and three for B2PLYP-D3 and PTPSS-D3). On the other hand, XYG3 and B2PLYP-D3 yield in 10 cases the worst MAD. PWPB95-D3 is slightly better (eight cases). PTPSS-D3 gives in four cases the worst MADs; B2GPPLYP-D3 and DSD-BLYP-D3 in one case each. For the application to new, hitherto unexplored chemical problems, the DSD-BLYP-D3 and PWPB95-D3 functionals seem to be a good choice. The WTMADs [for an (aug-)def2-QZVP basis] underline the general applicability of PWPB95-D3 and DSD-BLYP-D3: 1.6 kcal/mol for PWPB95-D3 and 1.5 kcal/mol for DSD-BLYP-D3. B2GPPLYP-D3 has a WTMAD of 1.7 kcal/mol. PTPSS-D3 and XYG3 have a WTMAD of 1.9 kcal/mol. B2PLYP-D3 follows with 2.0 kcal/mol.
- (2) Further studies of GMTKN30 with the (aug-)def2-TZVPP basis reveal that, except for PWPB95-D3, DHDFs are (due to the perturbative correction) more basis set dependent than hybrids. The WTMADs are still better than for hybrids but also closer to them than for (aug-)def2-QZVP. Although fitted with a quadruple- $\zeta$  basis set, PWPB95-D3 is the best DHDF at the triple- $\zeta$  level, the least basis set dependent one (the dependence is similar to that of hybrids) and the only functional yielding a WTMAD below 2 kcal/mol. The WTMAD for PWPB95-D3 is 1.8 kcal/mol. It is followed by DSD-BLYP-D3 with 2.0 kcal/mol and by B2GPPLYP-D3 with 2.2 kcal/mol. PTPSS-D3 and XYG3 yield 2.3 kcal/mol. B2PLYP has a WTMAD of 2.4 kcal/mol.
- (3) Calculated reaction enthalpies for the first CO dissociation in transition metal carbonyls by DHDFs and MP2 are larger than the experimental reference values. However, PWPB95-D3 is closest to experimental values with an error of about 3 kcal/mol (about 5–10% of  $D_e$ ). This is attributed to the smallest

amount of Fock-exchange compared to the other DHDFs. Only XYG3 fails to reproduce the trend of the dissociation enthalpies in the series of compounds.

- (4) The good performance of XYG3 for main group compounds can be explained by a large effective local correlation contribution. In contrast to claims in the literature,<sup>21–23,50</sup> we find that the “better orbitals” that are used for the evaluation of XYG3 are more influenced by the smaller Fock-exchange in B3LYP and not by a full semilocal correlation part as claimed in refs 21–23 and 50. A study of different functionals and comparisons with HF proved that functionals with less Fock-exchange have lower average single-particle gaps. This leads to higher correlation energies if the resulting orbitals are used in the perturbative treatment. Thus, XYG3 has effectively a higher perturbative contribution than, e.g., B2PLYP and B2GPPLYP. This higher nonlocality and a reduced amount of the over-repulsive Becke 1988 gradient correction explains the good behavior of XYG3 for noncovalent interactions in previous studies, in which only medium-sized systems were considered.<sup>21–23,50,85</sup> Asymptotically, it misses about 57% of the dispersion energy and is thus not recommended in its present form for the calculation of van der Waals interactions in large systems.

In summary, our investigations revealed that PTPSS-D3 and PWPB95-D3 are valuable new functionals. They have a better formal scaling with system size than other DHDFs. They are robust for main group chemistry and seem to perform better than other DHDFs for transition metal compounds. PWPB95-D3 is the best DHDF for applications at a triple- $\zeta$  level. It is also relatively straightforward to implement these functionals in standard electronic structure codes (for checking purposes, see the absolute energies of three systems in Table S22 in the Supporting Information) and to derive the corresponding analytical derivatives. A comparison of the two new proposals finally shows that PWPB95-D3 clearly outperforms PTPSS-D3 in four out of five different statistical analyses. Many times, it has better MADs for the GMTKN30 set. The WTMADs are significantly lower, particularly at the triple- $\zeta$  level. The PTPSS error for the dissociation enthalpies of transition metal carbonyls is almost halved by PWPB95. Furthermore, PWPB95-D3 is mathematically less complicated and depends on fewer parameters. Moreover, only PWPB95-D3 can compete with the recently proposed DSD-BLYP functional. It is expected to also be useful for cases in which LYP correlation is known to fail. We therefore suggest general usage of PWPB95-D3 for future applications. The GMTKN30 database proved to be a useful tool for evaluating DFT methods, and further investigations along these lines are currently undertaken in our laboratories.

**Acknowledgment.** This work was supported by the “Fonds der Chemischen Industrie” with a scholarship to L.G. and by the Deutsche Forschungsgemeinschaft in the framework of the SFB 858 (“Synergetische Effekte in der Chemie—Von der Additivität zur Kooperativität”). We thank C. Mück-Lichtenfeld for his technical assistance.

**Supporting Information Available:** The formula for calculating the weighted total mean absolute deviation (WT-MAD). Information about determining the  $s_6$  for various MP2 versions and the double hybrids (Table S1). Information about the parameters fit sets (Tables S2 and S3). Results for GMTKN30 with (aug-)-def2-QZVP (Tables S4–S11). Results for GMTKN30 with (aug-)-def2-TZVPP (Tables S12–S19). Results for dissociation reactions of transition metal carbonyls (Table S20). Results for the study of HF and KS orbitals for five different molecules (Table S21). Reference values of PTPSS and PWPB95 for checking purposes, in case the functionals are implemented into other electronic structure codes (Table S22). This material is available free of charge via the Internet at <http://pubs.acs.org>.

## References

- (1) Hohenberg, P.; Kohn, W. *Phys. Rev. B* **1964**, *136*, 864–871.
- (2) Kohn, W.; Sham, L. J. *Phys. Rev.* **1965**, *140*, A1133–A1138.
- (3) Parr, R. G.; Yang, W. *Density-Functional Theory of Atoms and Molecules*; Oxford University Press: Oxford, U. K., 1989.
- (4) Koch, W.; Holthausen, M. C. *A Chemist's Guide to Density Functional Theory*; Wiley-VCH: New York, 2001.
- (5) Dreizler, J.; Gross, E. K. U. *Density Functional Theory, An Approach to the Quantum Many-Body Problem*; Springer: Berlin, 1990.
- (6) Rappoport, D.; Crawford, N. R. M.; Furche, F.; Burke, K. Approximate Density Functionals: Which Should I Choose? In *Computational Inorganic and Bioinorganic Chemistry*; Solomon, E. I., Scott, R. A., King, R. B., Eds.; Wiley-VCH: New York, 2009; pp 159–172.
- (7) Grimme, S. *J. Chem. Phys.* **2006**, *124*, 034108.
- (8) Görling, A.; Levy, M. *Phys. Rev. B* **1993**, *47*, 13105–13113.
- (9) Görling, A.; Levy, M. *Phys. Rev. A* **1994**, *50*, 196–204.
- (10) Zhao, Y.; Lynch, B. J.; Truhlar, D. G. *J. Phys. Chem. A* **2004**, *108*, 4786–4791.
- (11) Zhao, Y.; Lynch, B. J.; Truhlar, D. G. *Phys. Chem. Chem. Phys.* **2005**, *7*, 43–52.
- (12) Ángyán, J. G.; Gerber, I. C.; Savin, A.; Toulouse, J. *Phys. Rev. A* **2005**, *72*, 012510.
- (13) Grimme, S.; Schwabe, T. *Phys. Chem. Chem. Phys.* **2006**, *8*, 4398–4401.
- (14) Tarnopolsky, A.; Karton, A.; Sertchook, R.; Vuzman, D.; Martin, J. M. L. *J. Phys. Chem. A* **2008**, *112*, 3–8.
- (15) Karton, A.; Tarnopolsky, A.; Lamere, J. F.; Schatz, G. C.; Martin, J. M. L. *J. Phys. Chem. A* **2008**, *112*, 12868–12886.
- (16) Sancho-García, J. C.; Pérez-Jiménez, A. J. *J. Chem. Phys.* **2009**, *131*, 084108.
- (17) Benighaus, T.; Lochan, R. C.; Chai, J.-D.; Head-Gordon, M. *J. Phys. Chem. A* **2008**, *112*, 2702–2712.
- (18) Graham, D. C.; Menon, A. S.; Goerigk, L.; Grimme, S.; Radom, L. *J. Phys. Chem. A* **2009**, *113*, 9861–9873.
- (19) Chai, J.-D.; Head-Gordon, M. *J. Chem. Phys.* **2009**, *131*, 174105.
- (20) Kozuch, S.; Gruzman, D.; Martin, J. M. L. *J. Phys. Chem. C* **2010**, *114*, 20801–20808.
- (21) Zhang, Y.; Xu, X.; Goddard, W. A., III. *Proc. Natl. Acad. Sci. U.S.A.* **2009**, *106*, 4963–4968.
- (22) Zhang, I. Y.; Luo, Y.; Xu, X. *J. Chem. Phys.* **2010**, *132*, 194105.
- (23) Zhang, I. Y.; Luo, Y.; Xu, X. *J. Chem. Phys.* **2010**, *133*, 104105.
- (24) Schwabe, T.; Grimme, S. *Phys. Chem. Chem. Phys.* **2007**, *9*, 3397–3406.
- (25) Neese, F.; Schwabe, T.; Grimme, S. *J. Chem. Phys.* **2007**, *126*, 124115.
- (26) Grimme, S.; Mück-Lichtenfeld, C.; Würthwein, E.-U.; Ehlers, A. W.; Goumans, T. P. M.; Lammertsma, K. *J. Phys. Chem. A* **2006**, *110*, 2583–2586.
- (27) Grimme, S.; Antony, J.; Schwabe, T.; Mück-Lichtenfeld, C. *Org. Biomol. Chem.* **2007**, *5*, 741–758.
- (28) Grimme, S.; Schwabe, T. *Acc. Chem. Res.* **2008**, *41*, 569–579.
- (29) Antony, J.; Grimme, S. *Phys. Chem. Chem. Phys.* **2008**, *10*, 2722–2729.
- (30) Schwabe, T.; Grimme, S. *Eur. J. Org. Chem.* **2008**, 5928–5935.
- (31) Schwabe, T.; Grimme, S. *J. Phys. Chem. A* **2009**, *113*, 3005–3008.
- (32) Korth, M.; Grimme, S. *J. Chem. Theory Comput.* **2009**, *5*, 993–1003.
- (33) Schwabe, T.; Grimme, S. *J. Phys. Chem. Lett.* **2010**, *1*, 1201–1204.
- (34) Grimme, S.; Djukic, J.-P. *Inorg. Chem.* **2010**, *49*, 2911–2919.
- (35) Goerigk, L.; Grimme, S. *J. Chem. Theory Comput.* **2010**, *6*, 107–126.
- (36) Grimme, S.; Neese, F. *J. Chem. Phys.* **2007**, *127*, 154116.
- (37) Goerigk, L.; Grimme, S. *J. Phys. Chem. A* **2009**, *113*, 767–776.
- (38) Goerigk, L.; Moellmann, J.; Grimme, S. *Phys. Chem. Chem. Phys.* **2009**, *11*, 4611–4620.
- (39) Goerigk, L.; Grimme, S. *J. Chem. Phys.* **2010**, *132*, 184103.
- (40) Vintonyak, V. V.; Warburg, K.; Kruse, H.; Grimme, S.; Hübel, K.; Rauh, D.; Waldmann, H. *Angew. Chem., Int. Ed.* **2010**, *49*, 5902–5905.
- (41) Huenerbein, R.; Schirmer, B.; Moellmann, J.; Grimme, S. *Phys. Chem. Chem. Phys.* **2010**, *12*, 6940–6948.
- (42) Krieg, H.; Grimme, S. *Mol. Phys.* **2010**, *108*, 2655–2666.
- (43) Grimme, S.; Antony, J.; Ehrlich, S.; Krieg, H. *J. Chem. Phys.* **2010**, *132*, 154104.
- (44) Grimme, S.; Kruse, H.; Goerigk, L.; Erker, G. *Angew. Chem., Int. Ed.* **2010**, *49*, 1402–1405.
- (45) Takatani, T.; Hohenstein, E. G.; Malagoli, M.; Marshall, M. S.; Sherrill, C. D. *J. Chem. Phys.* **2010**, *132*, 144104.
- (46) Grimme, S. *J. Chem. Phys.* **2003**, *118*, 9095–9102.
- (47) Jung, Y.; Lochan, R. C.; Dutoi, A. D.; Head-Gordon, M. *J. Chem. Phys.* **2004**, *121*, 9793–9802.
- (48) Almlöf, J. *Chem. Phys. Lett.* **1991**, *181*, 319–320.
- (49) Janesko, B. G.; Scuseria, G. E. *Phys. Chem. Chem. Phys.* **2009**, *11*, 9677–9686.



- (50) Zhang, I. Y.; Wu, J.; Xu, X. *Chem. Commun.* **2010**, 46, 3057–3070.
- (51) Prof. Stefan Grimme Research Web Site. <http://www.uni-muenster.de/Chemie.oc/grimme/en/index.html> (accessed December 2010).
- (52) Gilbert, T. M. *J. Phys. Chem. A* **2004**, 108, 2550–2554.
- (53) Jurecka, P.; Hobza, P. *Chem. Phys. Lett.* **2002**, 365, 89–94.
- (54) Halkier, A.; Helgaker, T.; Jørgensen, P.; Klopper, W.; Koch, H.; Olsen, J.; Wilson, A. K. *Chem. Phys. Lett.* **1998**, 286, 243–252.
- (55) Grimme, S. *Angew. Chem., Int. Ed.* **2006**, 45, 4460–4464.
- (56) Grimme, S. *RICC: A coupled-cluster program using the RI approximation*; University of Münster: Münster, Germany, 2007.
- (57) Pitonák, M.; Neogrády, P.; Cerný, J.; Grimme, S.; Hobza, P. *Chem. Phys. Chem.* **2009**, 10, 282–289.
- (58) Jurecka, P.; Sponer, J.; Cerný, J.; Hobza, P. *Phys. Chem. Chem. Phys.* **2006**, 8, 1985–1993.
- (59) Podesszwa, R.; Patkowski, K.; Szalewicz, K. *Phys. Chem. Chem. Phys.* **2010**, 12, 5974–5979.
- (60) Grimme, S.; Steinmetz, M.; Korth, M. *J. Org. Chem.* **2007**, 72, 2118–2126.
- (61) Steinmann, S. N.; Csonka, G.; Carminboeuf, C. *J. Chem. Theory Comput.* **2009**, 5, 2950–2958.
- (62) Hehre, W. J.; Ditchfield, R.; Radom, L.; Pople, J. A. *J. Am. Chem. Soc.* **1970**, 92, 4796–4801.
- (63) Radom, L.; Hehre, W. J.; Pople, J. A. *J. Am. Chem. Soc.* **1971**, 93, 289–300.
- (64) Wodrich, M. D.; Jana, D. F.; von Ragué; Schleyer, P.; Corminboeuf, C. *J. Phys. Chem. A* **2008**, 112, 11495–11500.
- (65) Tsuzuki, S.; Honda, K.; Uchimaru, T.; Mikami, M. *J. Chem. Phys.* **2006**, 124, 114304.
- (66) Goll, E.; Werner, H.-J.; Stoll, H. *Phys. Chem. Chem. Phys.* **2005**, 7, 3917–3923.
- (67) Ogilvie, J. F.; Wang, F. J. H. *J. Mol. Struct.* **1992**, 273, 277–290.
- (68) Ogilvie, J. F.; Wang, F. J. H. *J. Mol. Struct.* **1993**, 291, 313–322.
- (69) Runeberg, N.; Pyykö, P. *Int. J. Quantum Chem.* **1998**, 66, 131–140.
- (70) Zhao, Y.; Truhlar, D. G. *Theor. Chem. Acc.* **2008**, 120, 215–241.
- (71) Perdew, J. P.; Ruzsinszky, A.; Tao, J.; Staroverov, V. N.; Scuseria, G. E.; Csonka, G. *J. Chem. Phys.* **2005**, 123, 62201.
- (72) Grimme, S. *J. Comput. Chem.* **2006**, 27, 1787–1799.
- (73) Becke, A. D. *Phys. Rev. A* **1988**, 38, 3098–3100.
- (74) Lee, C.; Yang, W.; Parr, R. G. *Phys. Rev. B* **1988**, 37, 785–789.
- (75) Miehlich, B.; Savin, A.; Stoll, H.; Preuss, H. *Chem. Phys. Lett.* **1989**, 157, 200–206.
- (76) Grimme, S. *J. Comput. Chem.* **2004**, 25, 1463–1473.
- (77) Elstner, M.; Hobza, P.; Frauenheim, T.; Suhai, S.; Kaxiras, E. *J. Chem. Phys.* **2001**, 114, 5149–5155.
- (78) Raghavachari, K.; Trucks, G. W.; Pople, J. A.; Head-Gordon, M. *Chem. Phys. Lett.* **1989**, 157, 479–483.
- (79) Kendall, R. A.; Dunning, T. H.; Harrison, R. J. *J. Chem. Phys.* **1992**, 96, 6796–6806.
- (80) Werner, H.-J.; Knowles, P. J.; Lindh, R.; Manby, F. R.; Schütz, M.; Celani, P.; Korona, T.; Rauhut, G.; Amos, R. D.; Bernhardsson, A.; Berning, A.; Cooper, D. L.; Deegan, M. J. O.; Dobbyn, A. J.; Eckert, F.; Hampel, C.; Hetzer, G.; Lloyd, A. W.; McNicholas, S. J.; Meyer, W.; Mura, M. E.; Nicklaß, A.; Palmieri, P.; Pitzer, R.; Schumann, U.; Stoll, H.; Stone, A. J.; Tarroni, R.; Thorsteinsson, T. *MOLPRO*, version 2009.1. See <http://www.molpro.net> (accessed November 9, 2010).
- (81) Kabelác, M.; Valdes, H.; Sherer, E. C.; Cramer, C. J.; Hobza, P. *Phys. Chem. Chem. Phys.* **2007**, 9, 5000–5008.
- (82) Tkatchenko, A., Jr.; R. A. D.; Head-Gordon, M.; Scheffler, M. *J. Chem. Phys.* **2009**, 131, 094106.
- (83) Slater, J. C. *Phys. Rev.* **1951**, 81, 385–390.
- (84) Vosko, S. J.; Wilk, L.; Nusair, M. *Can. J. Phys.* **1980**, 58, 1200–1211.
- (85) Vázquez-Mayagoitia, A.; Sherrill, C. D.; Aprá, E.; Sumpter, B. G. *J. Chem. Theory Comput.* **2010**, 6, 727–734.
- (86) Tao, J.; Perdew, J. P.; Staroverov, V. N.; Scuseria, G. E. *Phys. Rev. Lett.* **2003**, 91, 146401.
- (87) Perdew, J. P.; Kurth, S.; Zupan, A.; Blaha, P. *Phys. Rev. Lett.* **1999**, 82, 2544–2547.
- (88) Perdew, J. P.; Burke, K.; Ernzerhof, M. *Phys. Rev. Lett.* **1996**, 77, 3865–3868.
- (89) Perdew, J. P.; Ruzsinszky, A.; Tao, J.; Csonka, G. I.; Scuseria, G. E. *Phys. Rev. A* **2007**, 76, 042506.
- (90) Perdew, J. P.; Ruzsinszky, A.; Csonka, G. I.; Constantin, L. A.; Sun, J. *Phys. Rev. Lett.* **2009**, 103, 026403.
- (91) Perdew, J. P. In *Proceedings of the 21st Annual International Symposium on the Electronic Structure of Solids*; Ziesche, P., Eschrig, H., Eds.; Akademie Verlag: Berlin, 1991; p 11.
- (92) Becke, A. D. *J. Chem. Phys.* **1996**, 104, 1040–1046.
- (93) Zhao, Y.; Truhlar, D. G. *J. Phys. Chem. A* **2005**, 109, 5656–5667.
- (94) Adamo, C.; Barone, V. *J. Chem. Phys.* **1998**, 108, 664–675.
- (95) Perdew, J. P.; Wang, Y. *Phys. Rev. B* **1992**, 45, 13244–13249.
- (96) TURBOMOLE: Ahlrichs, R. et al. Universität Karlsruhe: Karlsruhe, Germany, 2008. See <http://www.turbomole.com>. (accessed November 9, 2010).
- (97) Ahlrichs, R.; Bär, M.; Häser, M.; Horn, H.; Kölmel, C. *Chem. Phys. Lett.* **1989**, 162, 165–169.
- (98) Eichkorn, K.; Treutler, O.; Öhm, H.; Häser, M.; Ahlrichs, R. *Chem. Phys. Lett.* **1995**, 240, 283–289.
- (99) Hättig, C.; Weigend, F. *J. Chem. Phys.* **2000**, 113, 5154–5161.
- (100) Weigend, F.; Ahlrichs, R. *Phys. Chem. Chem. Phys.* **2005**, 7, 3297–3305.
- (101) Metz, B.; Stoll, H.; Dolg, M. *J. Chem. Phys.* **2000**, 113, 2563–2569.

- (102) Peterson, K. A.; Figgen, D.; Goll, E.; Stoll, H.; Dolg, M. *J. Chem. Phys.* **2003**, *119*, 11113–11123.
- (103) Weigend, F. *Phys. Chem. Chem. Phys.* **2002**, *4*, 4285–4291.
- (104) Weigend, F.; Häser, M.; Patzelt, H.; Ahlrichs, R. *Chem. Phys. Lett.* **1998**, *294*, 143–152.
- (105) Eichkorn, K.; Weigend, F.; Treutler, O.; Ahlrichs, R. *Theor. Chem. Acc.* **1997**, *97*, 119–124.
- (106) Becke, A. D. *J. Chem. Phys.* **1993**, *98*, 5648–5652.
- (107) Stephens, P. J.; Devlin, F. J.; Chabalowski, C. F.; Frisch, M. J. *J. Phys. Chem.* **1994**, *98*, 11623–11627.
- (108) Hyla-Kryspin, I.; Grimme, S. *Organometallics* **2004**, *23*, 5581–5592.
- (109) Schäfer, A.; Huber, C.; Ahlrichs, R. *J. Chem. Phys.* **1994**, *100*, 5829–5835.
- (110) Perdew, J. P. *Phys. Rev. B* **1986**, *33*, 8822–8824.
- (111) Kind, C.; Reiher, M.; Neugebauer, J.; Hess, B. A. *SNF*, version 2.2.1; Universität Erlangen: Erlangen, Germany, 2002.
- (112) Becke, A. D. *J. Chem. Phys.* **1993**, *98*, 1372–1377.
- (113) Stowasser, R.; Hoffmann, R. *J. Am. Chem. Soc.* **1999**, *121*, 3414–3420.
- (114) Peach, M. J. G.; Benfield, P.; Helgaker, T.; Tozer, D. J. *J. Chem. Phys.* **2008**, *128*, 044118.
- (115) Teale, A. M.; Coriani, S.; Helgaker, T. *J. Chem. Phys.* **2010**, *132*, 164115.
- (116) Curtiss, L. A.; Raghavachari, K.; Trucks, G. W.; Pople, J. A. *J. Chem. Phys.* **1991**, *94*, 7221–7230.
- (117) Parthiban, S.; Martin, J. M. L. *J. Chem. Phys.* **2001**, *114*, 6014–6029.
- (118) Zhao, Y.; Truhlar, D. G. *J. Phys. Chem. A* **2006**, *110*, 10478–10486.
- (119) Guner, V.; Khuong, K. S.; Leach, A. G.; Lee, P. S.; Bartberger, M. D.; Houk, K. N. *J. Phys. Chem. A* **2003**, *107*, 11445–11459.
- (120) Ess, D. H.; Houk, K. N. *J. Phys. Chem. A* **2005**, *109*, 9542–9553.
- (121) Dinadayalane, T. C.; Vijaya, R.; Smitha, A.; Sastry, G. N. *J. Phys. Chem. A* **2002**, *106*, 1627–1633.
- (122) Zhao, Y.; Lynch, B. J.; Truhlar, D. G. *J. Phys. Chem. A* **2004**, *108*, 2715–2719.
- (123) Zhao, Y.; González-García, N.; Truhlar, D. G. *J. Phys. Chem. A* **2005**, *109*, 2012–2018.
- (124) Neese, F.; Schwabe, T.; Kossmann, S.; Schirmer, B.; Grimme, S. *J. Chem. Theory Comput.* **2009**, *5*, 3060–3073.
- (125) Zhao, Y.; Tishchenko, O.; Gour, J. R.; Li, W.; Lutz, J. J.; Piecuch, P.; Truhlar, D. J. *J. Phys. Chem. A* **2009**, *113*, 5786–5799.
- (126) Curtiss, L. A.; Raghavachari, K.; Redfern, P. C.; Pople, J. A. *J. Chem. Phys.* **1997**, *106*, 1063–1079.
- (127) Johnson, E. R.; Mori-Sánchez, P.; Cohen, A. J.; Yang, W. *J. Chem. Phys.* **2008**, *129*, 204112.
- (128) Piacenza, M.; Grimme, S. *J. Comput. Chem.* **2004**, *25*, 83–99.
- (129) Woodcock, H. L.; Schaefer, H. F., III; Schreiner, P. R. *J. Phys. Chem. A* **2002**, *106*, 11923–11931.
- (130) Schreiner, P. R.; Fokin, A. A.; Pascal, R. A.; de Meijere, A. *Org. Lett.* **2006**, *8*, 3635–3638.
- (131) Lepetit, C.; Chermette, H.; Gicquel, M.; Heully, J.-L.; Chauvin, R. *J. Phys. Chem. A* **2007**, *111*, 136–149.
- (132) Lee, J. S. *J. Phys. Chem. A* **2005**, *109*, 11927–11932.
- (133) Bryantsev, V. S.; Diallo, M. S.; van Duin, A. C. T.; Goddard, W. A., III. *J. Chem. Theory Comput.* **2009**, *5*, 1016–1026.
- (134) Reha, D.; Valdes, H.; Vondrasek, J.; Hobza, P.; Abu-Riziq, A.; Crews, B.; de Vries, M. S. *Chem.—Eur. J.* **2005**, *11*, 6803–6817.
- (135) Gruzman, D.; Karton, A.; Martin, J. M. L. *J. Phys. Chem. A* **2009**, *113*, 11974–11983.
- (136) Csonka, G. I.; French, A. D.; Johnson, G. P.; Stortz, C. A. *J. Chem. Theory Comput.* **2009**, *5*, 679–692.
- (137) Wilke, J. J.; Lind, M. C.; Schaefer, H. F., III; Császár, A. G.; Allen, W. D. *J. Chem. Theory Comput.* **2009**, *5*, 1511–1523.

CT100466K